Imperial College London
Department of Physics

$\mathcal{PT}$-Symmetric Models in Classical and Quantum Mechanics

Bjorn Karl Berntson

September 2012

Supervised by Carl M. Bender

Submitted in part fulfilment of the requirements for the degree of
Master of Science in Theoretical Physics from Imperial College London

Abstract

Researchers have recently contended that the Hermiticity condition usually imposed on quantum mechanical observables is too restrictive. In this thesis we provide evidence for this contention through a discussion of the theory of generalized $\mathcal{PT}$-symmetric classical and quantum mechanics. The underlying principle of such systems is introduced by means of a simple classical mechanical laboratory experiment: a parity-symmetric pair of isotropic harmonic oscillators with equal and opposite loss and gain imposed. In the parameter space defined by the strengths of the coupling and the loss-gain paramter, there are two distinct regions separated by a phase boundary. In the first, *unbroken* regime, energy transfers between the two oscillators to produce secondary, *Rabi* oscillations. In the *broken* regime, the loss-gain parameter overwhelms the coupling and we see exponential decay in one oscillator and exponential growth in the other. The phase transition is observed by variation of the relevant parameters. This classical situation is analogous to the phase transition between real and complex eigenvalues in a quantum system defined by a $\mathcal{PT}$-symmetric Hamiltonian. To construct a viable physical theory from such a Hamiltonian, we must first restrict to the unbroken-$\mathcal{PT}$-symmetric vector subspace. Then, with appropriate modification of the underlying inner-product space, the theory is rendered self-adjoint and unitary. We detail these constructions and provide a number of examples, focusing on finite-dimensional and exactly-solvable models where the interesting features of $\mathcal{PT}$ are most transparently observed.

Contents

1. Introduction, some simple models, and experimental realizations **7**

1.1. An overview of $\mathcal{PT}$-symmetric theory 7

1.1.1. Quantum theory 8

1.1.2. Classical theory 10

1.1.3. Experiments 11

1.2. Hermiticity is too restrictive: an exactly soluble model 11

1.3. Features of $\mathcal{PT}$ quantum mechanics in a two-level system . . 15

1.4. Experimental realizations 19

2. $\mathcal{PT}$-symmetric classical mechanics: an experiment and discussion of generalized dynamics on Riemann surfaces **21**

2.1. $\mathcal{PT}$ phase transition in a simple mechanical system 21

2.1.1. Theoretical model 22

2.1.2. Numerical models 26

2.1.3. Experimental details 30

2.2. Classical mechanics on Riemann surfaces 33

2.2.1. Definitions and complex-analytic features 33

2.2.2. Generalized harmonic oscillator 35

2.2.3. Classical ix^3 model 35

2.3. Symplectic formulation of mechanics on complex manifolds . 36

3. $\mathcal{PT}$-symmetric quantum mechanics and generalizations **40**

3.1. Geometrical constructions on finite-dimensional Hilbert spaces 40

3.1.1. Hermitian, real quantum mechanics 40

3.1.2. $\mathcal{PT}$-symmetric reformulation 42

3.2. Extension to infinite-dimensional Hilbert spaces 44

4. Concluding remarks **47**

A. Runge-Kutta **48**

B. Some notes on the $\mathcal{P}$ and $\mathcal{T}$ operations **50**

B.0.1. $\mathcal{P}$ and $\mathcal{T}$ as Lorentz group elements 50

B.0.2. Parity on vectors and operators 51

B.0.3. Time-reversal on vectors and operators 51

Bibliography **53**

List of Figures

2.1. A schematic for a $\mathcal{PT}$ symmetric system. A sink and sink are located at equal distances of a from the origin. The system is *odd* with respect to parity $\mathcal{P}$ because it physically interchanges the individual subsystems and *odd* with respect to time reversal $\mathcal{T}$ as it turns the sink into a source and the source into a sink. Therefore the system is *even* with respect to $\mathcal{PT}$. 22

2.2. A picture of our experimental setup. Two metal 'bobs' are suspended from a loosely hanging string that provides a weak, adjustable coupling. At the top of each suspended string is a small metallic washer that interacts with the mounted magnets. In particular, the mounted light gates will cause cause the magnet on the left to fire and provide an impulse when the pendulum is swinging away from the magnet (loss) and the magnet on the right fires when the pendulum is swinging towards it (gain). 23

2.3. Numerical solution of the equations of motion (2.5) with $\lambda = 0$ and $g = 0.075$ and the initial conditions $q_1(0) = 1$, $q_2(0) = p_1(0) = p_2(0) = 0$. The initial conditions cause the systems to be completely out of phase. In addition to the primary oscillations, there are secondary Rabi power oscillations due to the coupling g. 25

2.4. Numerical solution of the equations of motion (2.5) with $\lambda = g = 0.075$ and the initial conditions $q_1(0) = 1$, $q_2(0) = p_1(0) = p_2(0) = 0$. We are in the broken regime, and the Rabi oscillations have vanished. This models ceases to be valid after a cutoff time $t_c \approx 25$. This is because the equations of motion fail to conserve energy. 26

2.5. An energy-time plot showing the unbounded growth of the energy for the system governed governed by (2.5) when the paramters $\lambda = g = 0.075$ and initial conditions $q_1(0) = 1$, $q_2(0) = p_1(0) = p_2(0) = 0$ are used. 27
2.6. Numerical solution of the equations of motion using the differential-difference equations that conserve energy. We have $\omega_{\text{Rabi}} > \omega$ so that the broken region is attained and no secondary oscillations are observed. Here the parameters are $r = 0.7$ and $g = 0.01$ and the initial conditions are $q_1(0) = 1$, $q_2(0) = p_1(0) = p_2(0) = 0$. 28
2.7. Numerical solution of the equations of motion using the differential-difference equations that conserve energy. We have $\omega_{\text{Rabi}} < \omega$ so we remain in the unbroken region but the Rabi oscillations do not go to zero (compare with Fig. 2.6). Here the parameters are $r = 0.97$ and $g = 0.05$ and the initial conditions are $q_1(0) = q_2(0) = p_1(0) = p_2(0) = 1$. 29
2.8. Experimental results from the unbroken region. No current is supplied to the magnets and the tension in the suspended string is 200g. We observe Rabi oscillations in qualitative agreement with the results in Fig. 2.3. Due to friction in system, a slight decay in the amplitudes is observed as time progresses. 30
2.9. Experimental results from an intermediate-unbroken region where the secondary Rabi oscillations do not go to zero. A current of approximately 6A is supplied to the electromagnets and the tension in the suspended string is 400g. The results are in qualitative agreement with the energy-conserving numerical model in Fig. 2.7. 31
2.10. Experimental results from the broken region. The current in the magnets is approximately 13A and the tension in the string is 600g. Rabi oscillations have been overcome by the electromagnet strength and we observe qualitative agreement with Fig. 2.6. 32

1. Introduction, some simple models, and experimental realizations

1.1. An overview of $\mathcal{PT}$-symmetric theory

It is conventionally assumed that a quantum mechanical Hamiltonian must be Hermitian to faithfully describe a physical system. A Hermitian Hamiltonian is self-adjoint with respect to the standard, Hermitian inner product of quantum mechanics. This is a sufficient condition for the reality of the energy spectrum. A Hamiltonian is Hermitian in this sense if and only if it is invariant under simultaneous matrix-transposition and complex conjugation; this is represented symbolically by $H^\dagger = H$. Recently this condition has been challenged as being too restictive. In a pair of seminal papers [3, 5], Bender and collaborators showed, using numerical, asymptotic, and semiclassical techniques, that the spectrum of

$$H = p^2 + x^2(\mathrm{i}x)^\epsilon \tag{1.1}$$

is real and positive for $\epsilon \geq 0$. These Hamiltonians can be viewed as complex deformations of the harmonic oscillator Hamiltonian, included in the class at $\epsilon = 0$. This result was later given formal proof [20] using techniques from the theory of integrable systems. The class of Hamiltonians is clearly not Hermitian, but posesses an antilinear $\mathcal{PT}$ symmetry—invariance under simultaneous space and time reversal. On this basis it was proposed that Hermiticity be replaced withthe weaker requirement of space-time reflection invariance.

1.1.1. Quantum theory

The most obvious difference between conventional Hermitian theories and more general, $\mathcal{PT}$-symmetric theories is found in the associated Sturm-Liouville problems. Deriving from the position space representation of the eigenvalue problem $H|\psi\rangle = E|\psi\rangle$, the second order differential equations are associated with the boundary conditions

$$\lim_{|x|\to\infty} \psi(x) = 0. \tag{1.2}$$

In standard quantum mechanics the contour of integration is taken to be the real axis. For the class of Hamiltonians (1.1), the Schrödinger equation is given by

$$-\frac{\mathrm{d}^2\psi}{\mathrm{d}x^2} + x^2(\mathrm{i}x)^\epsilon\psi = E\psi \tag{1.3}$$

with boundary conditions *generally* [21] imposed on a contour C in the complex plane. The countours are bounded by Stokes lines [13]. The apparent ambiguity associated with the infinity of admissable contours is resolved by analytically continuing (1.3) away from the familiar Harmonic oscillator equation obtained at $\epsilon = 0$ [5].

Outside the realm of associated differential equations (1.2), a replacement of the Hermiticity condition raises important interpretational issues in quantum theory. Because $\mathcal{PT}$ is an antilinear symmetry, $[H, \mathcal{PT}] = 0$ does not imply simultaneously diagonalizability. When an eigenstate of the Hamiltonian is simultaneously an eigenstate of $\mathcal{PT}$, the eigenvalues are real we call the symmetry *unbroken*; otherwise the symmetry is *broken* and the eigenvalues come in complex conjugate pairs. A similar situation is encountered in quantum electrodynamics when working in the Coulomb gauge. Namely, we obtain an unphysical longitudinal photon polarization that is removed by restricting to a physical Hilbert space [22].

Replacing the standard Hermitian inner product with the obvious choice

$$\langle\psi|\varphi\rangle_{\mathcal{PT}} = \int_C \mathrm{d}x\, [\mathcal{PT}\psi(x)]\varphi(x) \tag{1.4}$$

gives rise to an indefinite metric space (a *Kreĭn* [29], or possibly a *Pontryagin* [28] space). This inner product is invariant under time-translation and choice of representative in ray spaces. On unbroken eigenstates $|\psi_m\rangle$ of a

$\mathcal{PT}$-symmetric Hamiltonian, the inner product (1.4) is (under appropriate assumptions [2]) pseudo-orthonormal:

$$\langle\psi_m|\psi_n\rangle_{\mathcal{PT}} = (-)^m\delta_{mn}. \tag{1.5}$$

A similar issue in developing an positive-definite inner product on Dirac spinors was remedied by introduction of the charge conjugation operator γ_5 [46]. In order to preserve the attractive features of (1.4), modifications must be implemented by a symmetry of a Hamiltonian that is self-adjoint with respect to (1.4). Such an operator $\mathcal{C}$—so-called because it has similar properties to Dirac's charge conjugation matrix—that results in an orthonormal inner product has been discovered [26, 4]. It has a simple position space representation as a sum over energy eigenstates

$$\mathcal{C}(x,y) = \sum_m \psi_m(x)\psi_m(y). \tag{1.6}$$

This expression is very difficult to calculate exactly and perturbative methods must often be used [24, 25]. This operator is self-inverse, commutes with the Hamiltonian: $[H,\mathcal{C}] = 0$, and has eigenvalues

$$\mathcal{C}(x,y)\psi_m(x) = (-)^m\psi_m(y). \tag{1.7}$$

Redefining the inner product (1.4) using (1.7) renders the energy eigenstates orthonormal

$$\langle\psi|\varphi\rangle_{\mathcal{CPT}} = \int_C \mathrm{d}x\,[\mathcal{CPT}\phi(x)]\varphi(x) \tag{1.8}$$

$$\langle\psi_m|\psi_n\rangle_{\mathcal{CPT}} = \delta_{mn}. \tag{1.9}$$

Moreover, this formulation of generalized quantum mechanics contains the Hermiticity case as a limit [4]. In the imit

$$\lim_{\epsilon\to 0}\mathcal{C} = \mathcal{P} \tag{1.10}$$

so $\mathcal{CPT} = \mathcal{T}$ and the Hermitian inner product is recovered.

With these inner product space modifications, non-Hermitian but $\mathcal{PT}$ symmetric Hamiltonians have been applied to several interesting problems in mathematical physics. For example, an suitable theory of massive elec-

troweak interactions without the Higgs mechanism has been developed from a $\mathcal{PT}$-symmetric Hamiltonian density [35]. In quartic quantum field theory, Bender and Sarkar showed that inconsistency owing to the negative value of the coupling constant and the presence of complex energies in can be resolved by using $\mathcal{PT}$- symmetric methods [34]. In the context of general relativity, Mannheim has recently proposed that a $\mathcal{PT}$ symmetric model for conformal gravity resolves the dark matter problem [36].

Despite these successes, foundational issues remain. For example, recent work [23, 38] has demonstrated that the $\mathcal{C}$ operator is not necessarily bounded, in particular for the $\mathrm{i}x^3$ model obtained from (1.1) with $\epsilon = 1$. Researchers have also questioned whether a Hilbert space approach is necessary and considered the properties of $\mathcal{PT}$-symmetric Hamiltonians in indefinite metric spaces [27]. A generalization of $\mathcal{PT}$ symmetric Hamiltonian theory was given by Mostafazadeh in a series of papers [39, 40, 41]. It is shown here that $\mathcal{PT}$ symmetry is a specific example of a more general notion of pseudo-Hermiticity. A pseudo-Hermitian Hamiltonian satisfies

$$H^\dagger = \eta H \eta^{-1}, \tag{1.11}$$

where η is a linear Hermitian automorphism. For many $\mathcal{PT}$-symmetric systems, the choice $\eta = \mathcal{P}$ demonstrates the correspondence between pseudo-Hermiticity and $\mathcal{PT}$ symmetry, but this prescription is not general [39]. General pseudo-Hermitian systems have many of the same properties as $\mathcal{PT}$-symmetric systems, including a phase transition between real and complex conjugate pairs of eigenvalues, a natural indefinite inner product, and unitary invariance.

1.1.2. Classical theory

Interest remains in the underlying classical properties of $\mathcal{PT}$-symmetric Hamiltonians. Originally studied in conjunction with their quantum counterparts in the original papers of Bender, these objects are now studied in their own right. The presence of complex potential terms in the Hamiltonian necessitates trajectories that lie on multi-sheeted Riemann surfaces. In a single complex dimension, a $\mathcal{PT}$ symmetric orbit is symmetric about the imaginary x-axis, as $\mathcal{P}$ exchanges quadrants I, III and II, IV while $\mathcal{T}$ relects about the real x-axis. As in the case of $\mathcal{PT}$-symmetric Hamilto-

nian operators, there is a parametric phase transition between regions of unbroken and broken $\mathcal{PT}$ symmetry [30], with trajectories now playing the role of energy eigenstates. These classical systems have many intriguing properties. At the fundamental level, the underlying symplectic geometry requires reexamination [9] and dynamical properties depend on the Riemann surface (configuration space) on which the system is defined [37]. The classical dynamics of these systems exhibit many features hitherto found only in quantum systems such as tunneling [31] and the presence of conduction bands [32]. Remarkably, a generalized complex correpsondence principle can be established for such systems [33].

1.1.3. Experiments

Experiments on $\mathcal{PT}$-symmetric systems are a recent development in the field and provide strong evidence that the underlying theory is worth studying. The first experiments were performed in the field of optics, demonstrating the parametric phase transition in optical waveguide systems described by a non-Hermitian but $\mathcal{PT}$-symmetric optical Hamiltonian [18, 14]. Optics, and in particular optophotonics, remains as the most fertile testing ground for experimental realizations of $\mathcal{PT}$-symmetry [15, 16]. However, experiments have also been done in condensed matter [17] and classical electrodynamics [6]. Towards the end of this chapter we detail some of these experiments as motivation for conducting our own simple classical mechanical experiment in which the phase transition is observed.

1.2. Hermiticity is too restrictive: an exactly soluble model

Here we review the axioms of quantum mechanics and show that the Hermiticity condition included in these is two restrictive by use of an explicit integrable model. For nonrelativistic quantum mechanics, we have the four axioms:

1. The state of a system is given by an equivalence class of vectors $[|\psi\rangle]$

in a projective Hilbert space $P(\mathcal{H})$.[1,2]

2. The set of smooth[3] functions on a classical mechanical phase space, $C^\infty(\Gamma, \mathbb{R})$ ('physical observables'), corresponds to the set of self-adjoint[4] operators on the projective Hilbert space with respect to a *Hermitian*[5] inner product.

3. The eigenvalue problem $H|\psi\rangle = E|\psi\rangle$ for $H \in \hom P(\mathcal{H})$ determines the allowed states of the system.

4. A Lie group[6] $G = \{U : \mathbb{R} \to \hom P(\mathcal{H}) : UU^\dagger = U^\dagger U = 1\} \cong (\mathbb{R}, +)$ generates the dynamics of the system.

These axioms give rise to a mathematically-consistent theory. However, a subtle insufficiency in the second axiom has recently given rise to a flurry of research in fields from mathematical physics to integrable systems and spectral theory to experimental optics and condensed matter.

The insufficiency arises as follows. Given a Hermitian operator Ω on $P(\mathcal{H})$ it is trivial to show $\operatorname{spec}\Omega \subset \mathbb{R}$:

$$\langle H\psi|\varphi\rangle = \langle\psi|H\varphi\rangle \implies E^*\langle\psi|\varphi\rangle = E\langle\psi|\varphi\rangle \tag{1.12}$$

so $E^* = E \in \mathbb{R}$. This is a sufficient, *but not necessary*, condition for the reality of the spectrum, as I will show by explicit counterexample.

In this simple example we consider the Hamiltonian[7]

$$H = \sum_{(ij)\in S_3} L_{ij}^2 + \frac{\alpha q_3}{\sqrt{q_1^2 + q_2^2}} \tag{1.13}$$

[1] A Hilbert space is a Banach space (a complete normed vector space) in which the norm $\|\cdot\|$ derives from an inner product $\langle\cdot|\cdot\rangle$.

[2] $P(\mathcal{H}) \equiv (\mathcal{H}\backslash\{0\})/\sim$ where $\psi \sim \varphi$ if $\varphi = \alpha\psi$ with $\alpha \in \mathbb{C}$.

[3] For a complex manifold, we require *holomorphic* functions, so the set becomes $C^\omega(\Gamma, \mathbb{C})$.

[4] A linear operator $\Omega \in \hom P(\mathcal{H}) \equiv \hom(P(\mathcal{H}), P(\mathcal{H}))$ is self-adjoint with respect to $\langle\cdot|\cdot\rangle$ if $\langle\Omega\psi|\varphi\rangle = \langle\psi|\Omega\varphi\rangle\ \forall\psi, \varphi \in P(\mathcal{H})$.

[5] There is a discrepancy between the physics and mathematics literature as to what is meant by 'Hermitian.' In physics the word is used synonymously with 'self-adjoint'. In mathematics 'Hermitian' refers to a specific sesquilinear form (linear in the first argument, antilinear in the second). An operator is the Hermitian if it is self-adjoint with respect to the inner product derived from this form.

[6] Here we define $1 \equiv \mathrm{id}_{P(\mathcal{H})}$.

[7] S_3 is the permutation group on a set of three elements.

where L_{ij} are angular momenta and the classical system is defined on the cotangent bundle of the two-sphere $\Gamma = T^*S^2$ with $\alpha \in \mathbb{R}$. Following the deformation of H into a linear operator on the projectivization of $\mathcal{H} = L^2S^2$, we can construct a spectrum-generating Poisson algebra—the existence of such an algebra is closely related to the (super)integrability of the equations of motion [7, 8].

Under the commutator there are three quantum-conserved[8] constants of the motion

$$L_{12} = q_1\partial_2 - q_2\partial_1 \tag{1.14}$$

$$e_1 = L_{12}L_{23} + L_{23}L_{12} - \frac{\alpha q_1}{\sqrt{q_1^2 + q_2^2}} \tag{1.15}$$

$$e_2 = L_{12}L_{13} + L_{13}L_{12} - \frac{\alpha q_1}{\sqrt{q_2^2 + q_2^2}}, \tag{1.16}$$

subject to a Casimir relation

$$e_1^2 + e_2^2 + 4L_{12}^4 - 4HL_{12}^2 + H - 5L_{12}^2 - \alpha^2 = 0. \tag{1.17}$$

The vector $(e_1, e_2) \in \hom P(\mathcal{H}) \times \hom P(\mathcal{H})$ is an analogue of the Laplace-Runge-Lenz vector in the Kepler problem [43] because the basis $\{L_{12}, e_1, e_2\}$ generates the Poisson algebra

$$[L_{12}, e_1] = -e_2 \quad [L_{12}, e_2] = e_1 \quad [e_1, e_2] = 4(H - 2L_{12}^2)L_{12} + L_{12} \tag{1.18}$$

For convenience we make a $GL_3\mathbb{C}$ change of basis and define raising and lowering operators

$$e_+ = e_1 - \mathrm{i}e_2 \quad e_- = e_1 + \mathrm{i}e_2, \tag{1.19}$$

where we also define $e_0 = L_{12}$ and $\{e_0, e_+, e_-\}$ is understood to be a subset of $\hom P(\mathcal{H})$.

We now show that this choice of basis permits us to solve the eigenvalue problem in a manner analogous to the highest weight method in SU_2. Noting that a vanishing commutator between some f_i and H implies f_i is an endomorphism on $P(\mathcal{H})_E \equiv \{[|\psi\rangle] \in P(\mathcal{H}) : H|\psi\rangle = E|\psi\rangle, E \in \mathbb{R}\}$ and making the assumption that $\dim P(\mathcal{H})_E < \infty$ we give the Poisson algebra

[8] Here, quantum conservation means the *expectation value* of the operator is conserved.

and operators actions on $P\mathcal{H})_E$:

$$[e_0, e_\pm] = \pm e_\pm, \quad [e_+, e_-] = 8He_0 + 16e_0^3 + 2e_0 \tag{1.20}$$

$$e_0|\psi\rangle = \lambda|\psi\rangle, \quad e_0 e_\pm|\psi\rangle = (e_\pm e_0 \pm e_\pm)|\psi\rangle = (\lambda \pm 1)e_\pm|\psi\rangle. \tag{1.21}$$

The Casimir relation is now expressed as

$$e_+e_- = \alpha^2 + (4He_0 + 8e_0^3 + e_0) - (4e_0^4 + 4He_0^2 + H + 5e_0^2) \tag{1.22}$$

or

$$e_-e_+ = \alpha^2 - (4He_0 + 8e_0^3 + e_0) - (4e_0^4 + 4He_0^2 + H + 5e_0^2). \tag{1.23}$$

By our assumption of finite-dimensionality, we have

$$e_0 e_\pm^{n_\pm+1}|\psi\rangle \tag{1.24}$$

for some $n_\pm \in \mathbb{N}$. It follows that $\dim P(\mathcal{H})_E = n_+ + n_-$.

We label the states by their weights. Taking $[|\psi\rangle]$ as an arbitrary (nonzero by the projectivization of the Hilbert space) element of $P(\mathcal{H})_E$ we define the highest weight state by $|0\rangle = e_+^{n_+}|\psi\rangle$ and more generally for $k \in \mathbb{N}$ we define the state

$$|k\rangle = e_-^k|0\rangle. \tag{1.25}$$

Making use of the commutation relations for $k \in \{0, ..., n_+ + n_-\} \subset \mathbb{N}$

$$e_0 e_-^k|0\rangle = e_0|k\rangle = (\lambda + n_+ - k)|k\rangle \tag{1.26}$$

and recalling the Casimir relations (1.22-1.23) and applying them to the vectors $|0\rangle, |n_+ + n_-\rangle \in P(\mathcal{H})_E$ we obtain a system of equations

$$\begin{aligned} e_+|0\rangle =& [-(4E+1)(\lambda+n_+) - 8(\lambda+n_+)^3 - 4(\lambda+n_+)^4 \\ &- (4E+5)(\lambda+n_+)^2 - E + \alpha^2]|0\rangle = 0 \end{aligned} \tag{1.27}$$

$$\begin{aligned} e_-|n_+ + n_-\rangle =& [4(E+1)(\lambda-n_-) + 8(\lambda-n_-)^3 - 4(\lambda-n_-)^4 \\ &- (4E+5)(\lambda-n_-)^2 - E + \alpha^2]|n_+ + n_-\rangle = 0. \end{aligned} \tag{1.28}$$

The first equation gives the spectrum

$$E = -\frac{1}{4}[2(\lambda + n_+) + 1]^2 + \frac{1}{4} + \frac{\alpha^2}{[2(\lambda + n_+) + 1]^2} \tag{1.29}$$

which, upon substitution into (1.28), admits two solutions:

$$\lambda + n_+ = \frac{n_+ + n_-}{2}, \quad \lambda + n_+ = \frac{n_+ + n_- + \sqrt{(n_+ + n_- + 1)^2 + 2\mathrm{i}\alpha}}{2}. \tag{1.30}$$

Making the defintion $n \equiv n_+ + n_-$, we write down two the two spectra of our system, corresponding to distinct eigenspaces $P(\mathcal{H})_{E_n^1}$ and $P(\mathcal{H})_{E_n^2}$.[9]

$$E_n^1 = -\frac{1}{4}(n+1)^2 + \frac{1}{4} + \frac{\alpha^2}{(n+1)^2} \tag{1.31}$$

$$E_n^2 = -\frac{1}{4}\left(n + \sqrt{(n+1)^2 + 2\mathrm{i}\alpha}\right)^2 + \frac{1}{4} + \frac{\alpha^2}{\left(n + \sqrt{(n+1)^2 + 2\mathrm{i}\alpha}\right)^2} \tag{1.32}$$

Let us focus on the second result. If we choose $\alpha \in \mathbb{C}\backslash\mathbb{R} \cup \{0\}$ we still obtain a real spectrum. Evidently our restriction of α to $\mathbb{R}$ was too restrictive. Note that in this event, H is no longer Hermitian. However, it *is* $\mathcal{PT}$ symmetric. These discrete reflection operators, which will occupy central importance throughout this thesis, act on $P(\mathcal{H})$ (and $\hom P(\mathcal{H})$ in the adjoint representation) as

$$\mathcal{P} : q_i \to -q_i \quad p_i \to -p_i \tag{1.33}$$

$$\mathcal{T} : q_i \to \quad q_i \quad p_i \to -p_i \quad \mathrm{i} \to -\mathrm{i}. \tag{1.34}$$

1.3. Features of $\mathcal{PT}$ quantum mechanics in a two-level system

In the previous section we have demonstrated by explicit example that the usual Hermiticity requirement is not a necessary condition for the reality of an eigenvalue spectrum. There is much more to $\mathcal{PT}$ quantum mechanics than a modification of the Hermiticity condition!

First we note some elementary properties of $\mathcal{P}$ and $\mathcal{T}$. $\mathcal{P}$ is a unitary

[9] Which spectrum is obtained depends on the *boundary conditions* of the problem, now on the complex two sphere $S^2(\mathbb{C})$. This space has a distinct topology from $S^2(\mathbb{R})$.

operator, while $\mathcal{T}$ is an *antiunitary* operator[10] satsifying

$$\mathcal{P}^2 = 1, \quad \mathcal{T}^2 = 1, \quad [\mathcal{P}, \mathcal{T}] = 0. \tag{1.35}$$

Momentarily ignoring the antilinearity of $\mathcal{T}$, we give an incorrect (but illuminating) 'proof' of the reality of the eigenvalue spectrum of a $\mathcal{PT}$-symmetric Hamiltonian.

Let $[|\psi\rangle] \in \mathcal{H}\mathbb{P}$ and consider the eigenvalue problem $\mathcal{PT}|\psi\rangle = \lambda|\psi\rangle$. Left-multiplying this equation by $\mathcal{PT}$ and using (1.35) we obtain $|\psi\rangle = |\lambda|^2|\psi\rangle$ by the complex conjugation inherent in $\mathcal{PT}$. Thus $\operatorname{spec}\mathcal{PT} = \{e^{\mathrm{i}\theta} : \theta \in \mathbb{R}\} = S^1$. The assumption $[\mathcal{PT}, H] = 0$ applied to the eigenvalue problem $H|\psi\rangle = E|\psi\rangle$ yields

$$\begin{aligned} \mathcal{PT}H|\psi\rangle &= \mathcal{PT}|E\psi\rangle \\ H\mathcal{PT}|\psi\rangle &= E^*\mathcal{PT}|\psi\rangle \end{aligned} \tag{1.36}$$

so $\operatorname{spec} H \subset \mathbb{R}$. The flaw in this argument lies in the assumption that $[\mathcal{PT}, H]$ implies simultaneous diagonalizability because $\mathcal{T}$, and thusly $\mathcal{PT}$, is an *antilinear* operator. We must relegate simultaneous diagnolizability to an *assumption.*

Definition 1. *A quantum system defined by a $\mathcal{PT}$ symmetric Hamiltonian H is said to be in a $\mathcal{PT}$-unbroken state if $\mathcal{PT}|\psi\rangle = |\psi\rangle$ holds for $[|\psi\rangle] \in P(\mathcal{H})_E$. This, by the above 'proof,' guarantees the reality of the eigenvalue spectrum.*

Some natural questions arise. What are the properties of the $\mathcal{PT}$-*broken* region and how does it relate to the unbroken regime? In short, the unbroken and broken regions are separated by a phase boundary in parameter space. In the broken regime, complex-conjugate pairs of eigenvalues replace the real spectrum in the unbroken region. This is best illustrated by a simple (but nontrivial) matrix model. We will discuss the general theory of phase transitions and a physical interpretation of this system in the subsequent chapter.

Let us take the Hlibert space to be the Riemann sphere $\mathbb{CP} \equiv \mathbb{C} \cup \infty$

[10] Wigner showed that the use of unitary and antiunitary operators is the most general way to implement symmetries on a Hilbert space.

and work with a Hamiltonian in $GL_2\mathbb{C}$. On this space[11] $\mathcal{P}$ has a matrix representation

$$\mathcal{P} = \begin{pmatrix} 0 & 1 \\ 1 & 0 \end{pmatrix} \tag{1.37}$$

and $\mathcal{T}$ is simply complex conjugation. The Hamiltonian

$$H = \begin{pmatrix} \lambda e^{\mathrm{i}\phi} & g \\ g & \lambda e^{-\mathrm{i}\phi} \end{pmatrix} \tag{1.38}$$

with $\phi, g, \lambda \in \mathbb{R}$ fails to be Hermitian (invariant under simultaneous transposition and complex conjugation) unless $\phi = 0$ or $\phi = \pi$, but it does commute with $\mathcal{PT}$. Evaluating the the secular determinant $\det(H - I_2 E)$, and solving the resulting quadratic equation, we find that the eigenvalues are given by

$$E_\pm = \lambda \cos\theta \pm \sqrt{g^2 - \lambda^2 \sin^2\phi} \tag{1.39}$$

and the evident reality condition by

$$g^2 \geq \lambda^2 \sin^2\phi. \tag{1.40}$$

When the equality holds, this equation defines a phase boundary in $g - \lambda$ parameter space, separating the unbroken and broken $\mathcal{PT}$ regions.

Let us consider the eigenvectors of the system[12]

$$|\pm\rangle = \begin{pmatrix} 1 \\ -\mathrm{i}\frac{\lambda}{g}\sin\phi \pm \sqrt{1 - \frac{\lambda^2}{g^2}\sin^2\phi} \end{pmatrix} = \begin{pmatrix} 1 \\ \pm e^{\mp \mathrm{i}\alpha} \end{pmatrix} \tag{1.41}$$

which, upon multiplication by inessential overall phases and normalization, become

$$|\pm\rangle = \frac{1}{\sqrt{2\cos\alpha}} \begin{pmatrix} e^{\pm \mathrm{i}\frac{\alpha}{2}} \\ \pm e^{\mp \mathrm{i}\frac{\alpha}{2}} \end{pmatrix} \tag{1.42}$$

[11] See appendix for details.

[12] We have made the definition $\sin\alpha \equiv \frac{\lambda}{g}\sin\phi$.

With this result we compute[13]

$$\langle +|-\rangle = -\mathrm{i}\tan\alpha \tag{1.44}$$

so that the eigenvectors are *not* orthogonal unless $\alpha = 0$ or $\alpha = \pi$; in these cases the Hamiltonian is actually Hermitian. This is an indication that our theory is not yet axiomatically sound. Let us briefly review the ramifications of Hermiticity and how it leads to a a physically and mathematically consistent theory.

We showed above that a Hermitian Hamiltonian has a real spectrum. It also generates unitary dynamics because $H = H^\dagger$ implies $[H, H^\dagger] = 0$ so that

$$e^{\mathrm{i}H}e^{-\mathrm{i}H^\dagger} = 1. \tag{1.45}$$

Furthermore, when a sesquilinear form is Hermitian, it is an inner product, giving rise to the probabilistic interpretation of quantum mechanics. This, combined with unitary time-evolution, guarantees conservation of probability:

$$\langle\psi|U^\dagger U|\varphi\rangle = \langle\psi|\varphi\rangle. \tag{1.46}$$

In order to construct a physical theory, we will need to both introduce a new inner product on $P(\mathcal{H})$ and implement unitary dynamics on this space. These constructions will be treated completely in the third chapter. Presently we simply demonstrate their existence.

First we define a linear operator $\mathcal{C}$ by summing over outer products of energy eigenstates

$$\mathcal{C} \equiv \sum_{P(\mathcal{H})_E} \frac{\psi\psi^T}{\|\psi\|^2} \tag{1.47}$$

and use it to define a new inner product

$$\langle\psi|\varphi\rangle_{\mathcal{CPT}} \equiv \frac{(\mathcal{CPT}|\psi\rangle)^T|\varphi\rangle}{\|\psi\|\|\varphi\|} \tag{1.48}$$

[13]Because we have projectivized $\mathbb{C}^2$, we need to generalize the standard Hermitian inner product on that space so it is independent of choice of representative:

$$\langle\phi|\varphi\rangle = \frac{\phi^\dagger\varphi}{\|\phi\|\|\varphi\|}. \tag{1.43}$$

Using (1.42), we find, for our two-level system

$$\mathcal{C} = \begin{pmatrix} \mathrm{i}\tan\alpha & \sec\alpha \\ \sec\alpha & -\mathrm{i}\tan\alpha \end{pmatrix}. \tag{1.49}$$

A short computation shows

$$\mathcal{CPT}|\psi\rangle = \begin{pmatrix} \psi_1^*\sec\alpha + \mathrm{i}\psi_2^*\tan\alpha \\ \psi_2^*\sec\alpha - \mathrm{i}\psi_1^*\tan\alpha \end{pmatrix} \tag{1.50}$$

and we finally obtain

$$\langle\pm|\pm\rangle_{\mathcal{CPT}} = 1, \quad \langle+|-\rangle_{\mathcal{CPT}} = 0. \tag{1.51}$$

A further short computation verifies $[\mathcal{CPT}, H] = 0$, so $\langle\psi|\varphi\rangle_{\mathcal{CPT}}$ is time independent and the dynamics are unitary.

1.4. Experimental realizations

In the previous section we have demonstrated by example that dropping the Dirac hermiticity requirement in favor of the weaker condition of $\mathcal{PT}$ symmetry can lead to a mathematically satisfactory theory. We are immediately led to ask whether such Hamiltonians are physically realizable. Here we detail some of the recent work on this subject, focusing on two experiments in particular that inspired us to perform the experiment detailed in the next chapter. The first experimental observation of $\mathcal{PT}$ symmetry breaking was published by researchers in 2010 [14]. The equivalence of the paraxial equation of diffraction and the Schrödinger equation of quantum mechanics is employed to obtain an physical system described by a Hamiltonian with a complex potential term (E is the electric-field envelope, z is the coordinate along the axis of propagation, and x is the transverse coordinate):

$$\mathrm{i}\frac{\partial E}{\partial z} + \frac{\partial^2 E}{\partial x^2} + [n_{\mathrm{R}}(x) + \mathrm{i}n_{\mathrm{I}}(x)]E = 0, \tag{1.52}$$

where we have omitted some constants. The real and imaginary components of the optical potential, n_{R} and n_{I} are even and odd with respect to $\mathcal{P}$ ($x \to -x$), respectively. This renders the system $\mathcal{PT}$-symmetric.

If two parallel optical waveguides interact with a coupling constant κ and

experience equal and opposite loss and gain with strength γ, this gives rise to the equations

$$\mathrm{i}\frac{\mathrm{d}E_1}{\mathrm{d}z} - \mathrm{i}\frac{\gamma}{2}E_1 + \kappa E_2 = 0 \qquad \mathrm{i}\frac{\mathrm{d}E_2}{\mathrm{d}z} - \mathrm{i}\frac{\gamma}{2}E_2 + \kappa E_1 = 0 \tag{1.53}$$

for the electric-field envelopes E_1 and E_2. Under $\mathcal{P}$ ($z \to -z$) and $\mathcal{T}$, the equations are invariant. By finding the eigenvalues like we did in the previous section, the phase transition is shown to occur at $\frac{\gamma}{2\kappa} = 1$.

An experimental realization of the above equations (1.53) was created using Fe-doped $LiNbO_3$ with two channels. A real, symmetric index profile is provided by in-diffusion Ti[14], the loss is provided by 'two-wave mixing using the material's photorefractive nonlinearity,' and gain by optical pumping. In the $\mathcal{PT}$ broke regime, this system exhibits some fascinating features such as adjustable transverse energy flow and non-reciprocal beam propagation. In the unbroken regime, power oscillations between channels (in the intensity profile) of the beam will be observed irrespective of into which channel the beam was input. However, in the broken regime, regardless of which channel receives the incident beam, the intensity profile in the channel with loss will vanish and the intensity profile of the channel with gain will remain constant—no power oscillations occur.

A similar *classical* system has been constructed in 2011 by Schindler, et. al. [6]. Here, two standard LRC ciricuits are coupled by their inductors and subjected to equal and opposite loss and gain. Loss is provided by a resistor and gain is provided by an amplifier-resistor feedback loop. The equations for the time-dependent charges Q_i on the capacitors are written in terms of Q_i and associated canonical momenta. Using an exponential substitutions, the eigenvalues and consequently the phase boundary are calculated and then observed in experiment. In this thesis we make use of formal similarities between classical electrodynamical and classical mechanical systems and conduct an experiment in which nearly identical phenomena can be observed in a pair of alternately damped and driven coupled isotropic pendula.

[14] Because this experiment concerns the dynamics of a *pair* of waveguides, we want the profile to be $\mathcal{P}$-symmetric and not $\mathcal{T}$ symmetric so that the whole system is $\mathcal{PT}$-symmetric.

2. $\mathcal{PT}$-symmetric classical mechanics: an experiment and discussion of generalized dynamics on Riemann surfaces

While $\mathcal{PT}$ symmetry (as a field of research) was originally realized in quantum theory [5], there exist very simple (as evidenced by the experiments descibed in the previous chapter) classical analogues. Quantisation procedures allow us to identify non-Hermitian quantum systems with more classical analogues on Riemann surfaces.

In this chapter we will begin by describing an elementary experiment that demonstrates the classical parametric phase transition between states of unbroken and broken $\mathcal{PT}$ symmetry. This is done to provide an intuitive explanation of the principles of $\mathcal{PT}$ symmetry and make contact with the matrix models that we consider in this thesis.

In this classical regime, Hamilton's equations ensure that Hamiltonians with complex potentials will give rise to trajectories that venture into the complex domain. Thus, the *configuration* (or *base*) space for a one dimensional system is a Riemann surface. We will detail this constructions and consider some specific Hamiltonians.

2.1. $\mathcal{PT}$ phase transition in a simple mechanical system

The presence of complex eigenvalues in a quantum mechanical system is an indication that the system is thermodynamically open. Let us see why this is by considering a system consisting of a source and sink of equal and opposite powers, positioned equidistant from the origin. A schematic for the

system is detailed in Fig. 2.1. It should be noted that an experiment [19] involving two coupled microwave cavities provides a nice physical realization of this schematic.

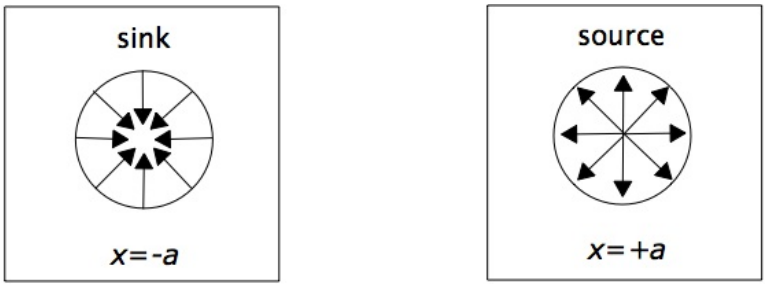

Figure 2.1.: A schematic for a $\mathcal{PT}$ symmetric system. A sink and sink are located at equal distances of a from the origin. The system is *odd* with respect to parity $\mathcal{P}$ because it physically interchanges the individual subsystems and *odd* with respect to time reversal $\mathcal{T}$ as it turns the sink into a source and the source into a sink. Therefore the system is *even* with respect to $\mathcal{PT}$.

2.1.1. Theoretical model

The Hamiltonian for the system in Fig. 2.1 is given by (1.38) with g set to zero—we are in the broken regime. This leads to the eigenvectors[1]

$$|\psi_L\rangle_0 = \begin{pmatrix} 1 \\ 0 \end{pmatrix} \quad |\psi_R\rangle_0 = \begin{pmatrix} 0 \\ 1 \end{pmatrix}. \tag{2.1}$$

The time dependent Schrödinger equation has solution $|\psi\rangle_t = e^{-\mathrm{i}Ht}|\psi\rangle_0$, leading to the time-dependent eigenvectors

$$|\psi_L\rangle_t = e^{-\mathrm{i}E_L t}\begin{pmatrix} 1 \\ 0 \end{pmatrix} \quad |\psi_R\rangle_t = e^{-\mathrm{i}E_R t}\begin{pmatrix} 0 \\ 1 \end{pmatrix}. \tag{2.2}$$

We see that the energies E_L, E_R must be a complex conjugate pair to generate the equal exponential decay and growth expected in the left and right systems, respectively. The above time-dependent eigenvectors of the Hamiltonian are not simultaneous eigenvectors of $\mathcal{PT}$ and the system is not in equilibrium. If we take g to be a sufficiently large real number, we can put

[1] The notation $|\pm\rangle$ for the eigenvectors is no longer appropriate and potentially confusing.

the system into the unbroken, *equilibrium* regime.

This system can be realized experimentally by a classical analogue. Here we consider two coupled oscillators: one with a energy source and the other with an energy sink. We have accomplished this by coupling two pendula with a string and using magnets to provide impulses to the pendula. Our experimental setup is detailed in Fig. 2.2.

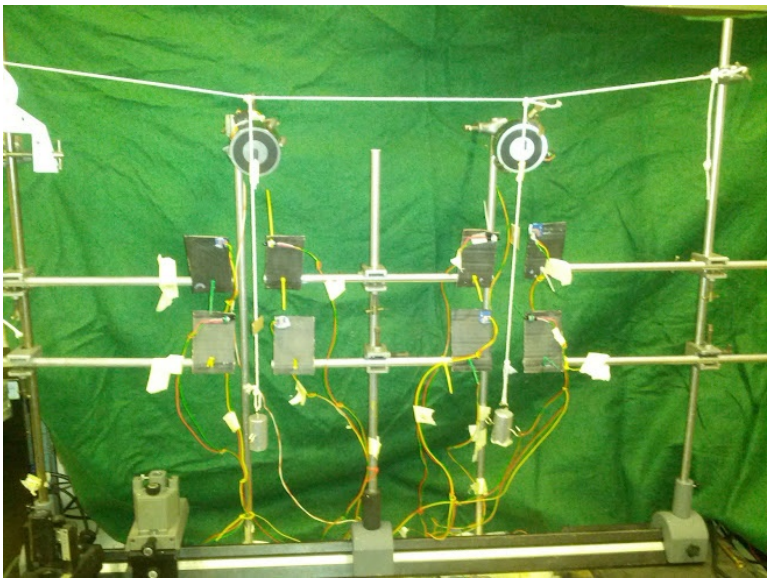

Figure 2.2.: A picture of our experimental setup. Two metal 'bobs' are suspended from a loosely hanging string that provides a weak, adjustable coupling. At the top of each suspended string is a small metallic washer that interacts with the mounted magnets. In particular, the mounted light gates will cause cause the magnet on the left to fire and provide an impulse when the pendulum is swinging away from the magnet (loss) and the magnet on the right fires when the pendulum is swinging towards it (gain).

This system is *open*; to obtain the equations of motion we will need to work from a basic oscillator Hamiltonian and implement the loss-gain mechanism into the resulting equations of motion. This Hamiltonian describing two isotropic coupled oscillators is given as

$$H = \frac{1}{2}p_1^2 + \frac{1}{2}p_2^2 + \frac{1}{2}\omega\left(q_1^2 + q_2^2\right) + gq_1q_2. \tag{2.3}$$

Because we are interested in qualitative agreement of our model with the

complicated dynamics of the system illustrated in Fig. 2.2, we wil work in units with ω set to unity to reduce the dimension of the parameter space. Then we obtain the equations of motion

$$\dot{q}_i = p_i, \quad \dot{p}_i = -q_i - g\mathcal{P}_{ij}q_j. \tag{2.4}$$

Now we implement the loss-gain mechanism by adding a term to the equations of motion

$$\dot{q}_i = p_i, \quad \dot{p}_i = -q_i - g\mathcal{P}_{ij}q_j - \lambda\varepsilon_{ij}p_j, \tag{2.5}$$

which are recast in matrix form as

$$\dot{\Psi} = L\Psi \tag{2.6}$$

with

$$\Psi = (q_1, q_2, p_1, p_2)^T \tag{2.7}$$

and

$$L = \begin{pmatrix} 0 & 0 & 1 & 0 \\ 0 & 0 & 0 & 1 \\ -1 & -g & -\lambda & 0 \\ -g & -1 & 0 & \lambda \end{pmatrix}. \tag{2.8}$$

By evaulating the secular determinant and setting the resulting quadratic form (in the *square* of the eigenvalue) to zero, we can determine the phase boundary between the unbroken and broken $\mathcal{PT}$ regimes.

$$\det\left(L - EI_4\right) = E^4 + (2-\lambda^2)E^2 + 1 - g^2 = 0 \tag{2.9}$$

$$E^2 = \frac{1}{2}\left(\lambda^2 - 2 \pm \sqrt{\lambda^4 - 4\lambda^2 + 4g^2}\right). \tag{2.10}$$

Two conditions must be satisfied to ensure the system is in the unbroken regime $E^2 < 0$.

$$\lambda^4 - 4\lambda^2 + 4g^2 > 0, \tag{2.11}$$

$$\lambda^2 - 2 + \sqrt{\lambda^4 - 4\lambda^2 + 4g^2} < 0. \tag{2.12}$$

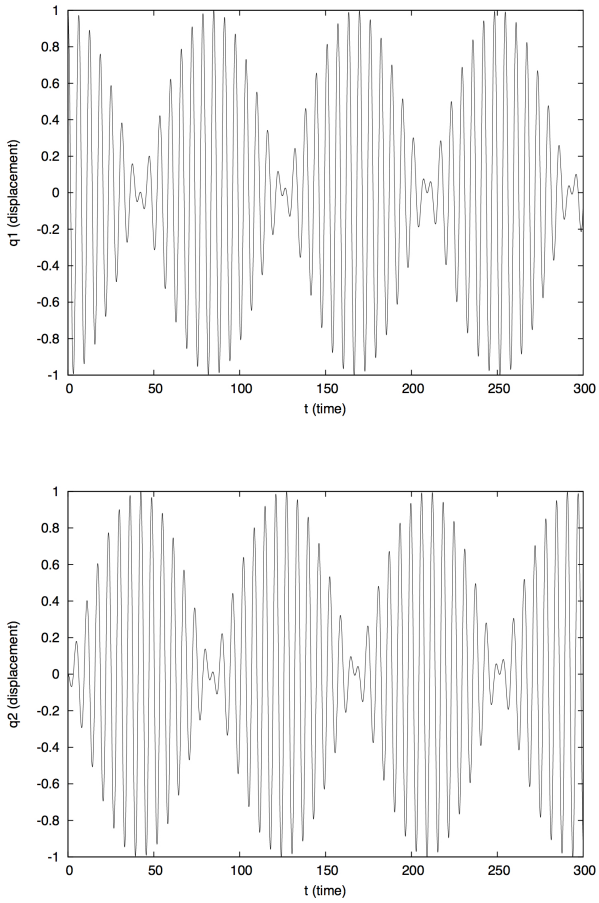

Figure 2.3.: Numerical solution of the equations of motion (2.5) with $\lambda = 0$ and $g = 0.075$ and the initial conditions $q_1(0) = 1$, $q_2(0) = p_1(0) = p_2(0) = 0$. The initial conditions cause the systems to be completely out of phase. In addition to the primary oscillations, there are secondary Rabi power oscillations due to the coupling g.

These conditions are combined to give

$$\lambda < 2\left(1 - \sqrt{1 - g^2}\right). \tag{2.13}$$

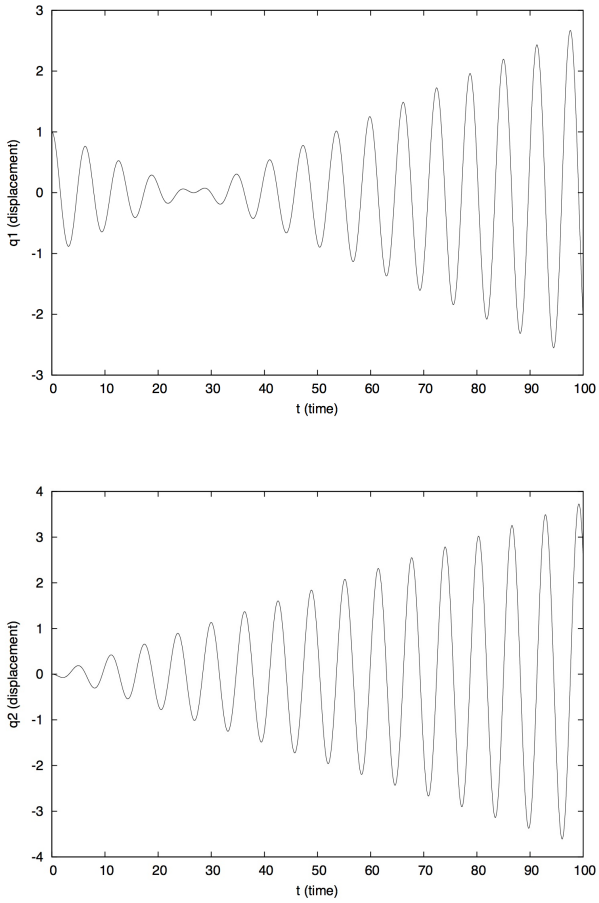

Figure 2.4.: Numerical solution of the equations of motion (2.5) with $\lambda = g = 0.075$ and the initial conditions $q_1(0) = 1$, $q_2(0) = p_1(0) = p_2(0) = 0$. We are in the broken regime, and the Rabi oscillations have vanished. This models ceases to be valid after a cutoff time $t_c \approx 25$. This is because the equations of motion fail to conserve energy.

2.1.2. Numerical models

We have implemented the equations of motion numerically using a fourth-order Runge-Kutta scheme[2] and have made use of (2.13) when searching the parameter space. When $\lambda = 0$, we simply have a system of coupled isotropic

[2]This scheme is detailed in the appendix.

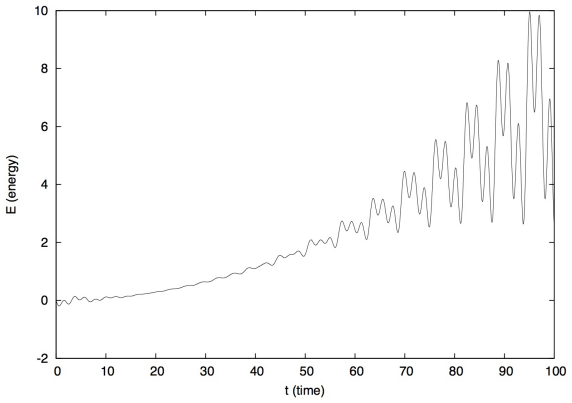

Figure 2.5.: An energy-time plot showing the unbounded growth of the energy for the system governed governed by (2.5) when the paramters $\lambda = g = 0.075$ and initial conditions $q_1(0) = 1$, $q_2(0) = p_1(0) = p_2(0) = 0$ are used.

harmonic oscillators as in Fig. 2.3. If the initial conditions are specified so the two subsystems are completely ($\frac{\pi}{2}$) out of phase, the parameter space of the system is reduced to a one-dimensional subset of the unbroken regime $(\mathbb{R}^+ \cup \{0\}) \times (\mathbb{R}^+ \cup \{0\}) \ni (g, \lambda)$. The motion of the system is characterized by the frequencies of the *primary* oscillations and *secondary* (*Rabi*) oscillations [48].

As we increase g from zero, the frequency of the Rabi oscillations increases until $\omega_{\text{Rabi}} = \omega$, at which point the broken $\mathcal{PT}$ region is attained. In this region our model will not conserve energy and both oscillators will grow out of bound after a cutoff time t_{c}. This is expected because the equations of motion do not follow from a Hamiltonian. As one oscillator is allowed to grow out of bounds, the energy it attains will leak into the paired oscillator. The result is that *both* oscillators grow out of bound and energy is not conserved as in Fig. 2.4.

A new model is required to describe our system—we will use a set of energy-conserving differential-difference equations. In this new model the results presented in Fig. 2.3 are preserved. We remove the terms in λ in (2.5) and begin with (2.4). At each maximum of q_1, we multiply the energy

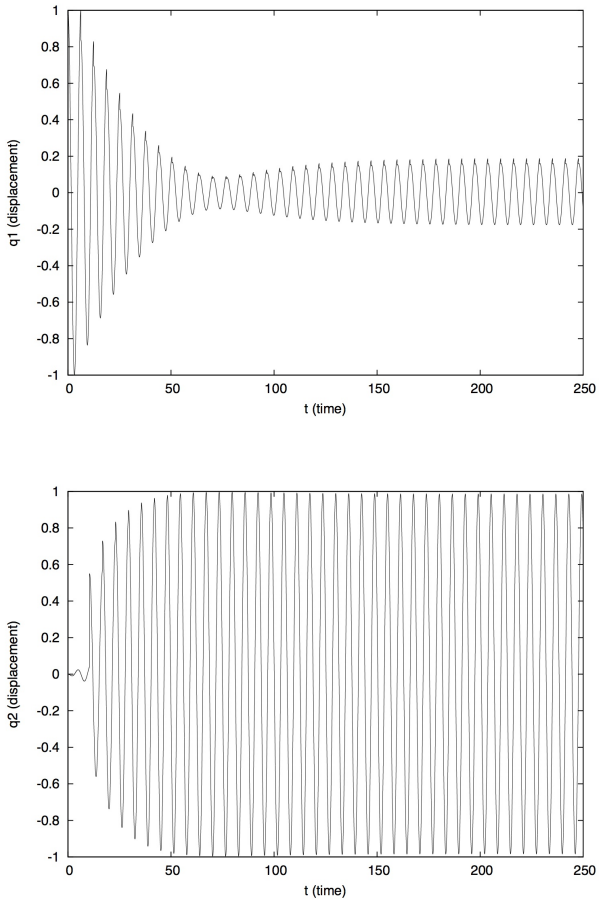

Figure 2.6.: Numerical solution of the equations of motion using the differential-difference equations that conserve energy. We have $\omega_{\text{Rabi}} > \omega$ so that the broken region is attained and no secondary oscillations are observed. Here the parameters are $r = 0.7$ and $g = 0.01$ and the initial conditions are $q_1(0) = 1$, $q_2(0) = p_1(0) = p_2(0) = 0$.

E_1 by a fixed number $r \in [0, 1]$, decrease the amplitude to compensate for the loss in energy, and reinitialize the simulation. At the subseqent maximum of q_2, we increase the energy E_2 by $(1-r)E_1$, increase the ampltitude correspondingly, and reinitialize the simulation. This gives a manifestly energy-conserving result for the broken regime, presented in Fig. 2.6. Our new numerical approach will conserve energy even for $r \neq 1$; we find in-

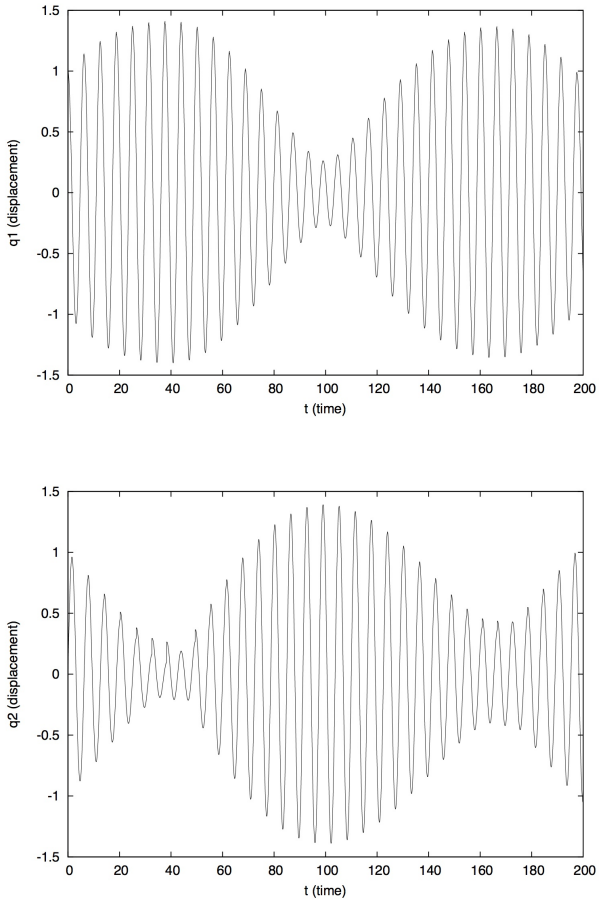

Figure 2.7.: Numerical solution of the equations of motion using the differential-difference equations that conserve energy. We have $\omega_{\text{Rabi}} < \omega$ so we remain in the unbroken region but the Rabi oscillations do not go to zero (compare with Fig. 2.6). Here the parameters are $r = 0.97$ and $g = 0.05$ and the initial conditions are $q_1(0) = q_2(0) = p_1(0) = p_2(0) = 1$.

teresting results in this unbroken region of the parameter space where the energy is not fully transferred between the subsystems. A graph of these results is presented in Fig. 2.7.

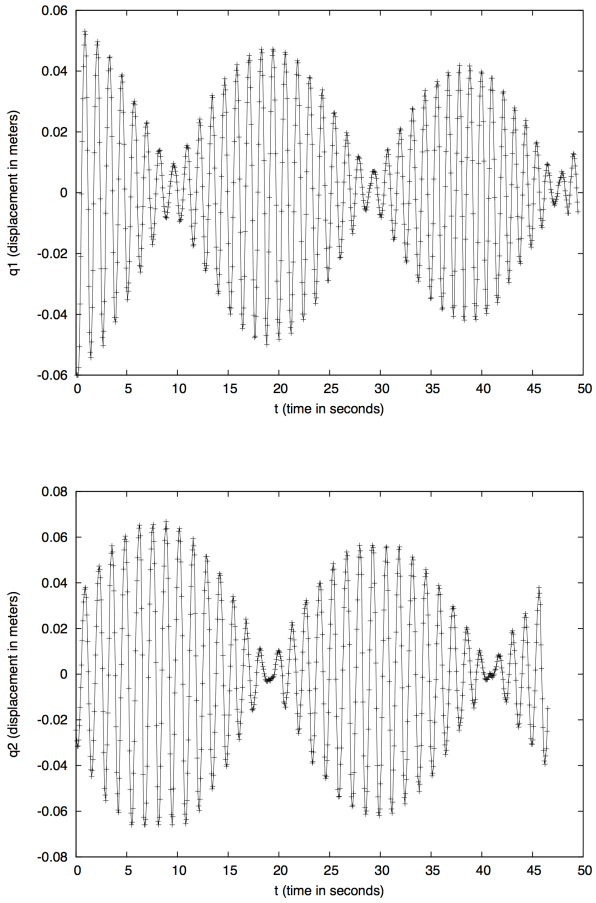

Figure 2.8.: Experimental results from the unbroken region. No current is supplied to the magnets and the tension in the suspended string is 200g. We observe Rabi oscillations in qualitative agreement with the results in Fig. 2.3. Due to friction in system, a slight decay in the amplitudes is observed as time progresses.

2.1.3. Experimental details

We have already presented a picture of our experimental setup in Fig.2.2. Here we provide some of the technical details needed to understand the experimental results and their relation to the numerical results in the previous section.

The system consists of two 50g metallic bobs suspended from a string

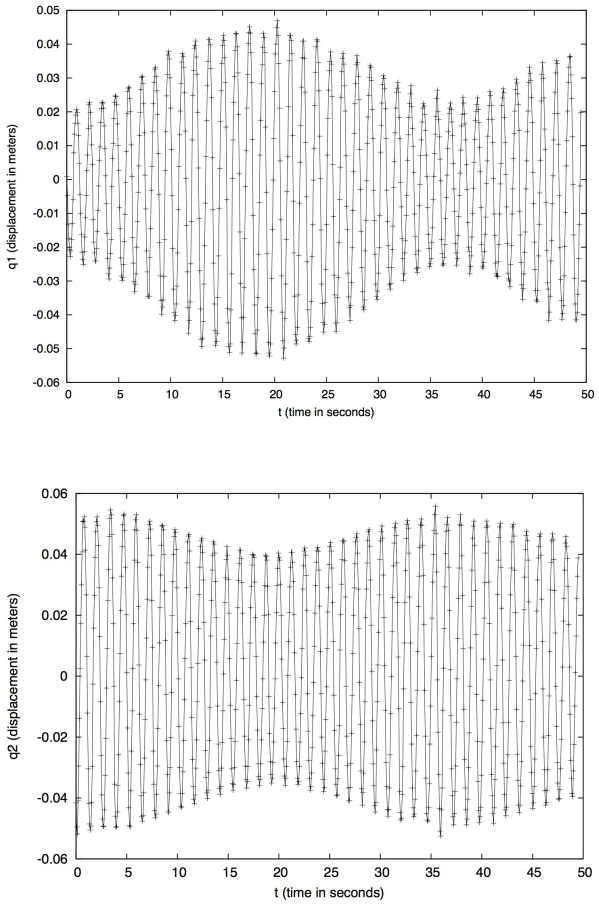

Figure 2.9.: Experimental results from an intermediate-unbroken region where the secondary Rabi oscillations do not go to zero. A current of approximately 6A is supplied to the electromagnets and the tension in the suspended string is 400g. The results are in qualitative agreement with the energy-conserving numerical model in Fig. 2.7.

of 39cm stretched between a pole and a wheel. The string is hung over the wheel and attached to a mass so that the tension (and consequently the coupling) of the system is adjustable. *A lower tension corresponds to a stronger coupling.* A pair of light gates are used in conjuction with ENABLE circuits to determine the direction that each pendulum swings. A larger circuit containing the ENABLE circuits directs a pair of magnets

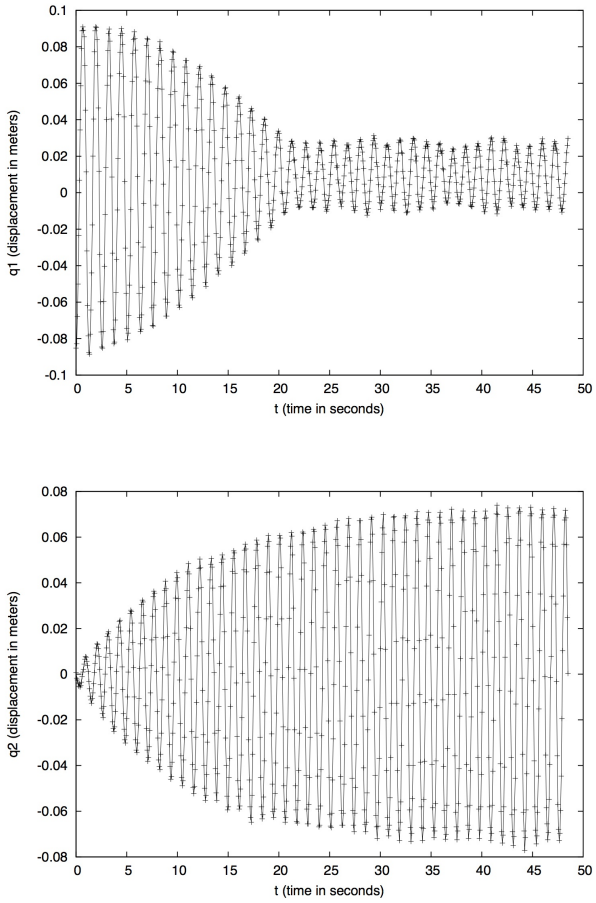

Figure 2.10.: Experimental results from the broken region. The current in the magnets is approximately 13A and the tension in the string is 600g. Rabi oscillations have been overcome by the electromagnet strength and we observe qualitative agreement with Fig. 2.6.

to fire—on the left, the magnet fires when the pendulum is swinging away so as to subtract energy; on the right, the magnet fires when the pendulum is swinging inwards to provide energy.

In the small angle approximation our systems should have good agreement with the improved, energy-conserving numerical model described in the previous section. We are able to record the motion of experiment using a video camera and motion-tracking software [50].

The first data is from the unbroken regime. We fix a mass of 200g to the suspended string and turn the magnets off. The results are presented in Fig. 2.8. We change the position in parameter space by increasing the tension to 400g and supplying a small current (∼6A) to the electromagnets. We remain in the unbroken regime, as illustrated in Fig. 2.9. Lastly, we increase both the current and the tension to ∼13A and 600g, respectively. This brings us into the broken regime, illustrated in Fig. 2.10.

The simple experiment we have described illustrates some of the general features of $\mathcal{PT}$-symmetric system, found in both experiment and theory and classical and quantum mechanical models. We next detail some of the classical mechanical theory.

2.2. Classical mechanics on Riemann surfaces

In the previous section we constructed theoretical and experimental models for a thermodynamically open, classical $\mathcal{PT}$-symmetric system. The analysis was possible in real variables. Now we will consider a class of Hamiltonian systems with complex potentials whose base space is generally a multi-sheeted Riemann surface.

2.2.1. Definitions and complex-analytic features

Definition 2. *A Riemann surface is a one dimensional complex manifold: a Hausdorff topological space M covered by sets $U_i \subseteq M$, $i \in I \subseteq \mathbb{Z}^+$ such that each set is associated with a homeomorphism $\phi_i : M \to \mathbb{C}$ to open sets of $\mathbb{C}$ (with respect to the metric topology) satisfying $\phi_{ij} \equiv \phi_i \circ \phi_j^{-1} \in C^\omega$ on each $U_i \cap U_j \neq \varnothing$.*

A general $\mathcal{PT}$ symmetric Hamiltonian on a base space of one complex dimension is written as

$$H = p^2 + V(q), \tag{2.14}$$

where $V \in C^\omega(X, \mathbb{C})$ satisfies $V^*(-q) = V(q)$. This relation is satisfed by the class of Hamiltonians

$$H = p^2 + q^2(\mathrm{i}q)^\epsilon \tag{2.15}$$

with $\epsilon \in \mathbb{R}\backslash\mathbb{R}^-$. Hamilton's equations take the form

$$\frac{\mathrm{d}q}{\mathrm{d}t} = \frac{\partial H}{\partial p} = 2p \tag{2.16}$$

$$\frac{\mathrm{d}p}{\mathrm{d}t} = -\frac{\partial H}{\partial q} = \mathrm{i}(2+\epsilon)(\mathrm{i}q)^{1+\epsilon}. \tag{2.17}$$

Solving for p in (2.15) and inserting the result into (2.16), we obtain a first-order equation in a single variable q:

$$\frac{\mathrm{d}q}{\mathrm{d}t} = \pm 2\sqrt{H - q^2(\mathrm{i}q)^\epsilon} \tag{2.18}$$

where we now interpret H as a real number. Under an appropriate scaling of the variables[3], this equation reduces to

$$\frac{\mathrm{d}q}{\mathrm{d}t} = \pm\sqrt{1 - q^2(\mathrm{i}q)^\epsilon}. \tag{2.19}$$

This function is associated with a multi-sheeted Riemann surface. The structure of this surface is determined by the branch cuts. Evidently there is a branch point at each solution to the equation

$$1 - q^2(\mathrm{i}q)^\epsilon = 0. \tag{2.20}$$

Using the polar representation for complex variables, we observe that $|q| = 1$ and $\arg q = \left\{0, \frac{2\pi}{2+\epsilon}, ..., \frac{2\pi(1+\epsilon)}{2+\epsilon}\right\}$. These are the classical turning points of the motion. There is an additional branch point at the origin when $\epsilon \notin \mathbb{Z}$. By defining the branch cuts to join the $\mathcal{PT}$ symmetric branch points and letting the branch cut at[4] $\frac{\pi}{2}$ extend to $\mathrm{i}\infty$, we ensure that the trajectories are localized to the principal sheet of the Riemann surface. In the event of a nonintegral ϵ, we define the branch cut at the origin to extend to $\mathrm{i}\infty$.

We will now consider the cases of $\epsilon = 0$ and $\epsilon = 1$. The first case is simply the harmonic oscillator and allows us to make contact with a well-known real classical mechanical system. The latter case is the classical analogue of the important quantum mechanical, $\mathcal{PT}$-symmetric $\mathrm{i}x^3$ model.

[3]For example, $q^2(\mathrm{i}q)^\epsilon \to Hq^2(\mathrm{i}q)^\epsilon$, $t \to 2\sqrt{H}t$.
[4]This occurs only when ϵ is odd.

2.2.2. Generalized harmonic oscillator

If we take $\epsilon = 0$ in (2.15), we have the familiar Hamilton equations for the harmonic oscillator. Here we treat the harmonic oscillator at an increased level of abstraction by allowing the initial position $q(0)$ to lie in a classically forbidden region (beyond the turning points ± 1 or in the complex plane). Even with this loosened restriction, the solution to Hamilton's equation take the familiar form

$$q(t) = \cos[\arccos q(0) \pm t] \tag{2.21}$$

$$p(t) = \mp \sin[\arccos q(0) \pm t] \tag{2.22}$$

and the trajectories $\gamma(t) = (q, p)(t)$ foliate the phase space $\mathbb{C} \times \mathbb{C}$. In particular, the solutions (2.22) separately foliate the position and momentum spaces $\mathbb{C}$ as ellipses.

Riemann surface issues are avoided by taking the only branch cut (see above discussion) to lie between the classical turning points [3]. The trajectories, being elliptical, are clearly left-right symmetric in the complex plane, and thus $\mathcal{PT}$ symmetric.

2.2.3. Classical $\mathrm{i}x^3$ model

Let us first note a peculiar feature of this model without solving any differential equations. We apply the Hamiltonian

$$H = p^2 + \mathrm{i}q^3 \tag{2.23}$$

to this system diagrammatically presented in Fig. 2.1. Let the left and right boxes extend along the negative real and postive real axis, respectively, with the source/sink strength parametrized by q^3. This physical description is $\mathcal{PT}$-symmetric and compatible with the above Hamiltonian. The the time required for a test particle to move between positive and negative infinity in this model is given by

$$\Delta t = \int_{\mathbb{R}} \frac{\mathrm{d}q}{p} = \int_{\mathbb{R}} \frac{\mathrm{d}q}{\sqrt{H - \mathrm{i}q^3}}. \tag{2.24}$$

This integral is convergent, so the system is in equilibrium and unbroken-$\mathcal{PT}$-symmetric. In fact, the obvious generalization of the integral (2.24)

$$\int_{\mathbb{R}} \frac{\mathrm{d}q}{\sqrt{H - q^2(\mathrm{i}q)^\epsilon}} \tag{2.25}$$

is convergent for $\epsilon \geq 0$, in agreement with the observations of Bender et. al. [3] and the proof by Dorey et. al. [20].

Let us return to the dynamics of this model. Now there are three turning points, the period of the orbits is a complicated expression involving gamma functions (as opposed to simply 2π for the elliptical trajectories on the harmonic oscillator), and the trajectories resemble cardioids [3]. For the purpose of our discussion, the most important new feature in this model is the existence of non-periodic motion. A test particle starting at the qualitatively new turning point on the imaginary q-axis travels up the associated branch cut to $\mathrm{i}\infty$ (in finite time! [3]), rendering the trajectory non-reversible and not $\mathcal{T}$ symmetric. Note that it remains $\mathcal{PT}$-symmetric. This is an example of $\mathcal{T}$ symmetry breaking *without* necessary $\mathcal{PT}$ symmetry breaking.

2.3. Symplectic formulation of mechanics on complex manifolds

A naive approach to formal classical mechanics on a complex manifold M is to construct the canonical cotangent bundle T^*M and equip it with the standard symplectic structure. Following Mostafazadeh [9], we show that this approach fails to produce the classical canonical commutation relations

$$\{q, H\} = \frac{\mathrm{d}q}{\mathrm{d}t} = \frac{\partial H}{\partial p} \tag{2.26}$$

$$\{p, H\} = \frac{\mathrm{d}q}{\mathrm{d}t} = -\frac{\partial H}{\partial q} \tag{2.27}$$

and that a new symplectic form is required.

Definition 3. *A symplectic structure on a manifold M is a closed, non-degenerate, globally-defined two-form $\omega \in \Omega^2 M$. Equivalently, a symplectic matrix is an antisymmetric element of the general linear group.*

Let $f, g \in C^\omega(T^*M; \mathbb{C})$. The Poisson bracket is defined in terms of the

symplectic form by[5]

$$\{f, g\} \equiv \iota_{X_f} \iota_{X_g} \omega \tag{2.30}$$

We define a multiplet as in (2.6) by

$$\xi = (q_1, ..., q_n, p_1, ..., p_n) \tag{2.31}$$

so that the Poisson bracket may be expressed as

$$\{f, g\} = \omega_{ij} \partial_{\xi_i} f \partial_{\xi_j} g. \tag{2.32}$$

The standard symplectic form on a manifold locally homeomorphic to[6] $\mathbb{R}^{2n}$ takes the form

$$\omega_{ij} = \begin{pmatrix} 0 & 1_n \\ -1_n & 0 \end{pmatrix}. \tag{2.33}$$

In our problem we work with coordinates $\xi_i = \mathrm{Re}\,\xi_i + \mathrm{i}\,\mathrm{Im}\,\xi_i$ and so that the corresponding differential operators are expressed as

$$\partial_{\xi_i} = \frac{1}{2}\left(\partial_{\mathrm{Re}\,q} + \mathrm{i}\partial_{\mathrm{Im}\,q_i}\right) \tag{2.34}$$

$$\partial_{\xi_i^*} = \frac{1}{2}\left(\partial_{\mathrm{Re}\,\xi_i} - \mathrm{i}\partial_{\mathrm{Im}\,\xi_i}\right). \tag{2.35}$$

Using the standard symplectic form (2.33) and the above identities, we write the Poisson bracket as

$$\{f, g\} = 2\sum_{i=1}^{n}\left(\partial_{\xi_i^*} f \partial_{\xi_{i+n}} g + \partial_{\xi_i} f \partial_{\xi_{i+n}^*} g - \partial_{\xi_{i+n}^*} f \partial_{\xi_i} g - \partial_{\xi_{i+n}} f \partial_{\xi_i^*} g\right). \tag{2.36}$$

Extending (2.14) to a configuration space of complex dimension n we

[5]The *interior product* is defined by

$$\iota_X : \Omega^p \to \Omega^{p-1} \tag{2.28}$$

$$\omega \mapsto \frac{1}{p!}\sum_{s=1}^{p}(-)^{s-1} X^{i_s} \omega_{i_1 ... i_s ... i_p} \mathrm{d}q^{i_1} \wedge ... \wedge \hat{\mathrm{d}q^{i_s}} \wedge ... \wedge \mathrm{d}q^{i_p} \tag{2.29}$$

where the $\hat{}$ denotes omission.

[6]The *real* dimension of the manifold is n and the *real* dimension of the fibre bundle is $2n$. The real dimensionality of these structures doubles when we allow our canonical coordinates to become complex.

obtain the Hamiltonian

$$H = \sum_{i=1}^{n} p_i^2 + V(q_1, ..., q_n) \tag{2.37}$$

where V is a holomorphic[7] function of the n complex variables q_i. Taking this as our Hamiltonian in (2.36), we compute

$$\dot{q_i} = \{q_i, H\} = 0 \tag{2.38}$$

$$\dot{p_i} = \{p_i, H\} = 0. \tag{2.39}$$

The standard symplectic form evidently fails to reproduce (2.26-2.27) and give the correct dynamics for our system. We will construct a new symplectic form by *beginning* with the relations (2.26-2.27) and postulating additional needed relations, by means of the reality condition

$$\{f, g\}^* = \{f^*, g^*\}. \tag{2.40}$$

In particular, we require

$$\{q_i, p_j\} = \delta_{ij} \tag{2.41}$$

$$\{q_i, q_j^*\} = \mathrm{i}\alpha\delta_{ij} \tag{2.42}$$

$$\{p_i, p_j^*\} = \mathrm{i}\beta\delta_{ij} \tag{2.43}$$

$$\{q_i, p_j^*\} = \gamma\delta_{ij} \tag{2.44}$$

with $\alpha, \beta \in \mathbb{R}$, $\gamma \in \mathbb{C}$. With respect to the multiplet (q_i, q_i^*, p_i, p_i^*), the symplectic matrix ω_{ij} takes the form

$$\omega_{ij} = \begin{pmatrix} 0 & -\mathrm{i}\alpha & -1 & -\gamma \\ \mathrm{i}\alpha & 0 & -\gamma^* & -1 \\ 1 & \gamma^* & 0 & -\mathrm{i}\beta \\ \gamma & 1 & \mathrm{i}\beta & 0 \end{pmatrix}. \tag{2.45}$$

[7] A holomorphic function of several complex variables is locally L^2 and satisfies the Cauchy-Riemann equations.

We define $g \in GL_4\mathbb{C}$ by

$$g_{ij} = \frac{1}{2}\begin{pmatrix} 1 & 1 & 0 & 0 \\ \mathrm{i} & -\mathrm{i} & 0 & 0 \\ 0 & 0 & 1 & 1 \\ 0 & 0 & \mathrm{i} & -\mathrm{i} \end{pmatrix}. \tag{2.46}$$

so that

$$g : (q_i, q_i^*, p_i, p_i^*)^T \mapsto (\operatorname{Im} q_i, \operatorname{Re} q_i, \operatorname{Re} p_i, \operatorname{Im} p_i)^T. \tag{2.47}$$

We conjugate ω in (2.45) by g to obtain the most general symplectic form for complexified dynamics in canonical coordinates.

$$\left(g\omega g^{-1}\right)_{ij} = \frac{1}{2}\begin{pmatrix} 0 & -\alpha & -1-\operatorname{Re}\gamma & \mathrm{i}\operatorname{Im}\gamma \\ \alpha & 0 & \mathrm{i}\operatorname{Im}\gamma & -1+\operatorname{Re}\gamma \\ 1+\operatorname{Re}\gamma & -\mathrm{i}\operatorname{Im}\gamma & 0 & -\beta \\ -\mathrm{i}\operatorname{Im}\gamma & 1-\operatorname{Re}\gamma & \beta & 0 \end{pmatrix}. \tag{2.48}$$

This matrix is clearly still symplectic. It is obviously antisymmetric, and a change of basis (similarity transformation) preserves the nonzero determinant of (2.45). Note that no choice of parameters can bring this matrix the form (2.33).

3. $\mathcal{PT}$-symmetric quantum mechanics and generalizations

In the previous section we demonstrated that the standard symplectic form for mechanics on a real manifold needed to be modified. Here we discuss the geometry of the Hilbert space structures in both standard, Hermitian quantum mechanics and generalized, $\mathcal{PT}$-symmetric quantum mechanics. We first discuss the appropriate formulation on finite-dimensional Hilbert spaces, following Bender et. al. [2], before generalizing to the infinite-dimensional spaces typically encountered in quantum mechanics. Finally we introduce some important models in this regime and consider some generalizations of $\mathcal{PT}$-symmetry such as pseudo-Hermiticity.

3.1. Geometrical constructions on finite-dimensional Hilbert spaces

We use a formulation of quantum mechanics often used in attempts to quantize gravity. The underlying symplectic and differential geometry is made manifest in this form. Moreover, we can see a clear disinction between Hermitian and $\mathcal{PT}$-symmetric quantum mechanics: the Hermitian theory can be posed on an real Hilbert space using appropriate geometrical objects, while the latter, generalized theory *requires* the complex field.

3.1.1. Hermitian, real quantum mechanics

For an ordinary, Hermitian system we equip the (real, projectivized) Hilbert space with a triple

$$(g, \omega, J) \in \mathcal{T}_2^0\mathcal{H} \times \mathcal{T}_2^0\mathcal{H} \times \mathcal{T}_1^1\mathcal{H} \tag{3.1}$$

where g is a postive-definite metric, ω is a symplectic form, and J is an *almost complex structure.*

Definition 4. *An almost complex structure on a Hilbert space $\mathcal{H}$ is a real, globally defined tensor satisfying*

$$J^a{}_c J^c{}_b = -\delta^a_b. \tag{3.2}$$

The triple (3.1) is required to satisfy the compatibility conditions.

$$J^a{}_c g_{ab} J^b{}_d = g_{cd} \tag{3.3}$$

$$\omega_{ab} = g_{ac} J^c{}_b. \tag{3.4}$$

With these compatible structures, the inner Hermitian product takes the form

$$\langle\psi|\varphi\rangle_g \equiv \frac{1}{2\|\psi\|_g\|\varphi\|_g}(g_{ab} - \mathrm{i}\omega_{ab})\psi^a\varphi^b. \tag{3.5}$$

It is easiest to study the adjointness properties of operators if we write (3.5) in terms of projection operators onto positive and negative J subspaces of $\mathcal{H}$:

$$\langle\psi|\varphi\rangle_g = \frac{1}{\|\psi\|_g\|\varphi\|_g} g_{ab}(P_{+J})^a{}_c\psi^c(P_{-J})^b{}_d\varphi^d \tag{3.6}$$

where

$$(P_{\pm J})^a{}_b = \frac{1}{2}(\delta^a_b \pm \mathrm{i}J^a{}_b). \tag{3.7}$$

Note that complex numbers come into the picture in the definition of the inner product and for convenience when introducing the above projection operators. The theory is well-defined on just the underlying real Hilbert space!

Using the representation of the inner product (3.6), we observe that an operator $\Omega^a{}_b$ is self-adjoint (Hermitian) if and only if $\Omega_{ab} = g_{ac}\Omega^c{}_b$ is symmetric and J-invariant:

$$\langle\psi|\Omega|\varphi\rangle = \frac{1}{\|\psi\|_g\|\varphi\|_g}\Omega_{ab}(P_{+J})^a{}_c\psi^c(P_{-J})^b{}_d\varphi^d \tag{3.8}$$

$$= \frac{1}{\|\psi\|_g\|\varphi\|_g} g_{ac}F^c{}_b(P_{+J})^a{}_c\psi^c(P_{-J})^b{}_d\varphi^d \tag{3.9}$$

$$= \frac{1}{\|\psi\|_g\|\varphi\|_g} g_{ab}F^a{}_c(P_{+J})^a{}_c\psi^c(P_{-J})^b{}_d\varphi^d. \tag{3.10}$$

3.1.2. $\mathcal{PT}$-symmetric reformulation

The geometry required to describe a non-Hermitian, but $\mathcal{PT}$-symmetric system is much more elaborate. In particular, the Hamiltonian becomes an intrinsic part of the structure, determining compatibility conditions for the structure (3.1) and two additional tensors (π and c) we will find necessary to add. We first give a formal definition before explicating the purpose of the new tensors and compatibility conditions. We require a 6-tuple

$$(g, \omega, J, \pi, c, H) \in \left(\mathcal{T}_2^0(\mathcal{H} \otimes \mathbb{C})\right)^2 \times \left(\mathcal{T}_1^1(\mathcal{H} \otimes \mathbb{C})\right)^4 \tag{3.11}$$

on a complexified Hilbert space. Here π is the parity operator (a representation of $\mathcal{P}$, c is a representation of the $\mathcal{C}$ operator mentioned in the first chapter, and H is a $\mathcal{PT}$-symmetric Hamiltonian.

π is an symmetry operator in the Hermitian formulation, according to the discussion above. Here it takes a more prominent role and will replace g for many purposes. This is reflected in the compatibility conditions

$$\pi_{ac}\pi^{cb} = \delta_b^a \tag{3.12}$$

$$J^a{}_c g_{ab} J^b{}_d = g_{cd} \tag{3.13}$$

$$\omega_{ab} = \pi_{ac} J^c{}_b \tag{3.14}$$

A naive replacement of g with π leads to inconsistency. In particular, the inner product

$$\langle\psi|\varphi\rangle_\pi \equiv \frac{1}{2\|\psi\|_\pi \|\varphi\|_\pi}(\pi_{ab} - \mathrm{i}\omega_{ab})\psi^a \varphi^b \tag{3.15}$$

is associated with a pseudo-norm; π_{ab} is not a positive-definite quadratic form. We can remove the indefiniteness by introducing the $\mathcal{C}$ operator. To do this we need to first consider a Hamiltonian—with which the $\mathcal{C}$ operator must be compatible. While self-adjoint operators with respect to (3.5) were derived from symmetric elements of the tensor space $\mathcal{T}_2^0$, self-adjoint operators with respect to (3.15) are derived from Hermitian elements of the space $\mathcal{T}_2^0(\mathcal{H} \otimes \mathbb{C})$. The relaxation of the self-adjointness condition as described above in terms of real symmetric $(0, 2)$ tensors necessitates that we allow complex operators and thus unlderlying complex vectors. Self-adjoint operators now satisfy :

$$\Omega^a{}_b = \pi^{ac}\Omega_{bc} \tag{3.16}$$

where

$$\Omega_{ab} = \bar{\Omega}_{ba}. \tag{3.17}$$

This is verified by a calculation identical to (3.8-3.10) and equivalent to the condition

$$\pi_{ad}\bar{\Omega}^{a}{}_{b}\pi^{bc} = \Omega^{c}{}_{d} \tag{3.18}$$

which we recognize as $\mathcal{PT}$ symmetry. Let us work with a Hamiltonian satisfying (3.18). The eigenvalue equation reads

$$H^{a}{}_{b}\psi^{b} = E\psi^{a} \tag{3.19}$$

and defines a subspace $\{\psi\} \subset \mathcal{H} \otimes \mathbb{C}$. This subspace may itself be decomposed into two subspaces—one with real eigenvalues (*unbroken regime*), and one with complex conjugate pairs of eigenvalues (*broken regime*). A necessary and sufficient condition for an energy eigenstate to have a real energy eigenvalue is for it to be an eigenstate of the $\mathcal{PT}$ operator

$$\pi^{a}{}_{b}\bar{\psi}^{b} = \lambda\psi^{a}. \tag{3.20}$$

We showed in the introduction that λ is a phase. If (3.20) and (3.19) hold, we use the $\mathcal{PT}$-symmetry condition on the Hamiltonian (3.18) to write

$$\pi^{a}{}_{c}\bar{H}^{c}{}_{d}\pi^{d}{}_{b}\psi^{b} = E\psi^{a}. \tag{3.21}$$

Complex-conjugating (3.21) and multiplying by $\pi^{e}{}_{a}$ to obtain a Kronecker delta, then substituting (3.20), we obtain

$$H^{a}{}_{b}\psi^{b} = \bar{E}\psi^{a} \tag{3.22}$$

which, along with (3.19), guarantees that E is real.

We now consider the $\mathcal{PT}$ norms of these states. Using (3.20), we have

$$\|\psi\|_{\pi}^{2} = \frac{1}{2}\pi_{ab}\psi^{a}\bar{\psi}^{b} = \frac{1}{2}g_{ab}\psi^{a}\psi^{b} \tag{3.23}$$

Due to (3.12), $\pi^{a}{}_{b}$ can be diagonalized with entries ± 1. A convenient assumpton of tracelessness

$$\pi^{a}{}_{a} = 0 \tag{3.24}$$

ensures that the signature of $\pi^a{}_b$ is split. Thus

$$\|\psi\|_\pi^2 = \pm 1 \tag{3.25}$$

on g-normalized energy eigenstates in the unbroken regime. Half of the states have positive norm and half have negative norm. It is shown in [2] that if $g_{ac}H^c{}_b$ is a symmetric tensor, energy eigenstates in the unbroken regime will be pseudo-orthogonal. This is however not a necessary condition. From hereon we make the assumption that unbroken energy eigenstates are pseudo-orthonormal with respect to (3.15):

$$\langle\psi_i|\psi_j\rangle_\pi = \frac{1}{2\|\psi_i\|_g\|\psi_j\|_g}\pi_{ab}\psi_i^a\psi_j^b = (-)^i\delta_{ij} \tag{3.26}$$

by choice of ordering of the set $\{\psi_i\}$ indexed by $I \subset \mathbb{Z}^+$. To ghostbust the states of negative norm, we consider the operator $c^a{}_b$ subject to the compatibility conditions

$$\pi_{ad}\bar{c}^a{}_b\pi^{bc} = c^c{}_d \tag{3.27}$$

$$H^a{}_c c^c{}_b = c^a{}_c H^c{}_b. \tag{3.28}$$

Making the definition

$$c^a{}_b\psi_i^b = (-)^i\phi_i^a, \tag{3.29}$$

we introduce the inner product

$$\langle\psi|\varphi\rangle_{c\pi} = \frac{1}{\|\psi\|_g\|\varphi\|_g}g_{ac}c^c{}_b\pi^b{}_d\psi^a\bar{\varphi}^b \tag{3.30}$$

which is seen to be orthonormal ($\langle\psi_i|\psi_j\rangle = \delta_{ij}$) on unbroken regime energy eigenstates by application of (3.29) and (3.26).

3.2. Extension to infinite-dimensional Hilbert spaces

We provide a brief extension to the typical infinite-dimensional spaces of quantum mechanics; this extension is generally straightforward. We now work with an intrisically complex projective Hilbert space and pose the

eigenvalue problem

$$H|\psi\rangle = E|\psi\rangle \tag{3.31}$$

for a non-Hermitian, but $\mathcal{PT}$-symmetric Hamiltonian. We work in position space —where $\mathcal{P} = \delta(x+y)$ and $\mathcal{T}$ is complex conjugation—so the eigenvalue problem becomes

$$-\frac{\mathrm{d}^2\psi}{\mathrm{d}x^2} + V\psi = E\psi, \tag{3.32}$$

where V is a $\mathcal{PT}$-symmetric potential. By studying the asymptotic behavior of the potential function, we determine the Stokes lines associated with the Sturm-Liouville problem (3.32) and can impose appropriate boundary conditions on a countour C in the complex plane. If the $\mathcal{PT}$-symmetry is unbroken, we have a set $\{|\psi_i\rangle\}$ of energy eigenstates satisfying both

$$H|\psi_i\rangle = E_i|\psi_i\rangle \tag{3.33}$$

and

$$\mathcal{PT}|\psi\rangle = |\psi\rangle \tag{3.34}$$

where, as in (1.42), we have absorbed an inessential overall phase into the state vector. Then, with respect to the $\mathcal{PT}$ inner product

$$\langle\psi|\varphi\rangle_{\mathcal{PT}} = \frac{1}{|||\psi|||\varphi|||}\int_C \mathrm{d}x(\mathcal{PT}\psi)\varphi, \tag{3.35}$$

the energy eigenstates are pseudo-orthonormal

$$\langle\psi_i|\psi_j\rangle = (-)^i\delta_{ij}. \tag{3.36}$$

The situation is remedied by introducing the $\mathcal{C}$ operator in the position basis as

$$\mathcal{C}(x,y) = \sum_i \psi_i(x)\psi_i(y). \tag{3.37}$$

Using the completeness relation (which has only be verified numerically [49])

$$\sum_i (-)^i\psi_i(x)\psi_j(y) = \delta(x-y), \tag{3.38}$$

it is verified that $\mathcal{C}(x,y)$ is self-inverse and commutes with $\mathcal{PT}$. $\mathcal{C}(x,y)$ also

commutes with the Hamiltonian and has eigenvalues

$$\mathcal{C}(x,y)\psi_i(y) = (-)^i\psi_i(x) \tag{3.39}$$

by our demand. These conditions are sufficient to calculate $\mathcal{C}$ perturbatively [24]. As in the finite dimensional case, the $\mathcal{CPT}$ inner product

$$\int_C \mathrm{d}x(\mathcal{CPT}\psi)\varphi \tag{3.40}$$

is then positive definite and unitary-invariant.

4. Concluding remarks

In this thesis we have provided a intuitive introduction to non-Hermitian but $\mathcal{PT}$ symmetric systems through a laboratory experiment and explicit models. One overriding goal of this project was to argue that $\mathcal{PT}$ symmetric theories deserve to be taken seriously, as they produce *interesting* models that can be *experimentally realized*. I have sought to demonstrate this through my personal interests in integrable models and geometry. Such models also connect smoothly with the experiment we discussed at length.

I will take the opportunity here to provide some information about current projects that have not yet reached publishable form. Firstly, we have been investigating the properties of extended systems of coupled oscillators: a chain of $\mathcal{PT}$-symmetric dimers. It is predicted that a system such as this may exhibit mechanical birefringence. We have developed numerical models to search the paramter space and have found promising behavior, but have not fully characterized the properties of the system. Secondly, we have been working on a C^* algebra formulation for $\mathcal{PT}$-symmetric quantum mechanics. This is absent from the literature and may resolve some of the foundational issues discussed in the introduction.

I would like to thank my supervisor, Carl M. Bender for piquing my interest in $\mathcal{PT}$ symmetry and providing support and encouragement throughout the course of this project. I would also like to thank my other collaborators, David Parker and E. Samuel, for their contributions to the experiment described in this thesis. Lastly, I wish to thank E. Roy Pike for useful discussion and the use of his laboratory at King's College London.

A. Runge-Kutta

Consider a (generally non-autonomous) first-order ordinary differential equation for a function $y : \mathbb{R} \to \mathbb{R}$.

$$y = f(y, x) \tag{A.1}$$

Given the value of y at a point x_0, we wish to find the value at a point $x_0 + h$. A Runge-Kutta scheme of arbitary order expresses this new value as

$$y(x + h) \approx y(x) + hw_i z_i \tag{A.2}$$

with summation implied. Here the w_i are weights and the z_i are samples defined by

$$z_i = f[y(x) + h\alpha_{ij} z_j, x + \beta_i h]. \tag{A.3}$$

Because the z_i are defined recursively, the matrix α_{ij} must be strictly lower triangular. We choose to sample points at the starting point x, the midpoint $x + \frac{1}{2}h$, and the endpoint $x + h$. For a fourth order scheme, this correpsonds to the choice

$$\alpha_{21} = \alpha_{32} = \frac{1}{2},\ \alpha_{43} = 1 \tag{A.4}$$

$$\beta_1 = 0,\ \beta_2 = \beta_3 = \frac{1}{2},\ \beta_4 = 1, \tag{A.5}$$

though other choices are possible.

The samples become

$$z_1 = f[y(x), x] \tag{A.6}$$

$$z_2 = f\left[y(x) + \frac{1}{2}hz_1, x + \frac{1}{2}h\right] \tag{A.7}$$

$$z_3 = f\left[y(x) + \frac{1}{2}hz_2, x + \frac{1}{2}h\right] \tag{A.8}$$

$$z_4 = f[y(x) + hz_3, x + h] \tag{A.9}$$

Noting $y'(x) = f(y, x)$ and using the chain rule repeatedly to order $O(h^2)$, we can express (A.2) as an expansion in partial x-derivatives of f to order $O(h^5)$. The algebra required to do this is formidable and is omitted. Comparing the result to the Taylor expansion of $y(t + h)$ to the same order:

$$y(x+h) = y(x)+hf[y(x), x]+\frac{h^2}{2}f_t[y(x), x)]+\frac{h^3}{6}f_{tt}[y(x), x]+\frac{h^4}{24}f_{ttt}[y(x), x]+O(h^5), \tag{A.10}$$

a system of equations for the weights w_i is obtained with solution

$$w_1 = w_4 = \frac{1}{6},\ w_2 = w_3 = \frac{1}{3}. \tag{A.11}$$

Thus, we recover the familiar formula

$$y(t + h) = \frac{1}{6}(z_1 + 2z_2 + 2z_3 + z_4) \tag{A.12}$$

for the z_i defined above. The extension to a system of differential equations is straightforward by promoting y to a vector y_i and allowing the functions f_i to depend on that vector.

B. Some notes on the $\mathcal{P}$ and $\mathcal{T}$ operations

B.0.1. $\mathcal{P}$ and $\mathcal{T}$ as Lorentz group elements

It is perhaps best to start with a discussion of the discrete operators $\mathcal{P}$ and $\mathcal{T}$ in the context of the Lorentz group $O_{3,1}$. We can decompose this group as

$$O_{3,1} = L_+^\uparrow \cup L_+^\downarrow \cup L_-^\uparrow \cup L_-^\downarrow \tag{B.1}$$

where $L_+^\uparrow \cup L_+^\downarrow \equiv SO_{3,1}$ and $L_+^\uparrow$ is the proper, octochronous Lorentz group. More generally, $\operatorname{sgn}\det\Lambda$ is represented by $\pm$ and $\operatorname{sgn}\Lambda^0{}_0$ is represented by $\uparrow,\downarrow$ [44]. A relativistic field theory is required to be invariant under $L_+^\uparrow$, but not necessarily the whole group $O_{3,1}$. $\mathcal{P}$, $\mathcal{T}$ and $\mathcal{PT}$ are not necessary symmetries of a theory,[1] but discrete, additional symmetries that have definite consequences. The whole group $O_{3,1}$ preserves the Minkowski metric

$$g_{\mu\nu} = \operatorname{diag}(1,-1,-1,-1). \tag{B.2}$$

In terms of the action on four-vectors x^μ, $\mathcal{P} \in L_-^\uparrow$ is represented by the matrix

$$\mathcal{P}_{\mu\nu} = \operatorname{diag}(1,-1,-1,-1) \tag{B.3}$$

and corresponds to spatial inversion, while $\mathcal{T} \in L_-^\downarrow$ is represented by

$$\mathcal{T}_{\mu\nu} = \operatorname{diag}(-1,1,1,1). \tag{B.4}$$

and corresponds to time inversion.

Conjugation by $\mathcal{P}$ maps $L_+^\updownarrow \leftrightarrow L_-^\updownarrow$ while conjugation by $\mathcal{T}$ maps $L_\pm^\uparrow \leftrightarrow L_\pm^\downarrow$. In order to implement parity and time-reversal on quantum mechanical fields and operators, we need to find a representation for $\mathcal{P}$ and $\mathcal{T}$ as

[1] However, $\mathcal{CPT}$ is [**?**]

(anti)unitary operators.

B.0.2. Parity on vectors and operators

The construction for spinor fields is detailed in [46]; here we focus on nonrelativistic quantum mechanics. In particular, we consider $|\psi\rangle \in \mathcal{H}$—for sake of definiteness we take $\mathcal{H} = L^2(\mathbb{R}^n)$— and expand in the position basis.

$$|\psi\rangle = \int_{\mathbb{R}^n} \mathrm{d}^n x |x\rangle\langle x|\psi\rangle \tag{B.5}$$

It is now straightforward to implement space inversion:

$$U(\mathcal{P})|\psi\rangle = \int_{\mathbb{R}^n} \mathrm{d}^n x |-x\rangle\langle x|\psi\rangle. \tag{B.6}$$

Changing the variable of integration to $(-x)$ and left multiplying by the bra $|x\rangle$, we obtain

$$U(\mathcal{P})\psi(x) \equiv \langle x|U(\mathcal{P})|\psi\rangle = \psi(-x). \tag{B.7}$$

Applying parity twice, we verify that $U(\mathcal{P})$ is Hermitian, unitary, self-inverse, and has eigenvalues of precisely ± 1. If we expand (B.7) in the momentum basis we obtain

$$\langle x|U(\mathcal{P})|\psi\rangle = \int_{\mathbb{R}^n \times \mathbb{R}^n} \mathrm{d}^n x \, \mathrm{d}^n p \, \langle x|U(\mathcal{P})|p\rangle\langle p|\psi\rangle = \langle -x|\psi\rangle. \tag{B.8}$$

To obtain the desired delta function in the integral to make the equation true, we must have

$$U(\mathcal{P})|p\rangle = |-p\rangle. \tag{B.9}$$

Thus, momentum inversion is a necessary consequence of spatial inversion. We implement parity on operators in the usual way

$$U(\mathcal{P})H(x,p)U(\mathcal{P}) = H(-x,-p) \tag{B.10}$$

B.0.3. Time-reversal on vectors and operators

Implementing time-reversal in this context is less straightforward than implementing parity because we cannot expand in a natural basis. Nontheless it can be done easily by inspection of the Schrödinger equation [11] or the propagator [46]. Here we follow the latter approach. Let $\psi(x^\mu)$ be a solution

of the free Dirac theory. Then we must have

$$\psi(t, x^i) = e^{\mathrm{i}Ht}\psi(x^i)e^{\mathrm{i}Ht}. \tag{B.11}$$

Assuming time-reversal symmetry of the Hamiltonian, we apply time-reversal to both sides and right-multiply by a zero-energy vaccuum $|0\rangle$,

$$\psi(-t, x^i)|0\rangle = e^{\mathrm{i}Ht}\mathcal{T}\psi(x^i)\mathcal{T}|0\rangle. \tag{B.12}$$

Expanding the left side in terms of the vacuum, we obtain an inconsistency:

$$e^{-\mathrm{i}Ht}\psi(x^i)|0\rangle = e^{\mathrm{i}Ht}\mathcal{T}\psi(x^i)\mathcal{T}|0\rangle. \tag{B.13}$$

Namely, the left side is a sum of positive frequency terms while the right is a sum of negative frequency terms. This is surmounted by requiring that $\mathcal{T}$ perform complex conjugation:

$$\mathcal{T}z\mathcal{T} = \bar{z} \tag{B.14}$$

for $z \in \mathbb{C}$. Twofold application of $\mathcal{T}$ verifies that it has the same algberaic properties as parity, with unitarity replaced by antiunitarity. Examining the momentum operator

$$p^i = -\mathrm{i}\partial^i, \tag{B.15}$$

we see that momentum is reversed, while the position operator carries no imaginary unit and thus is preserved. On an operator $H(x, p)$ we have

$$\mathcal{T}H(x, p)\mathcal{T} = H^*(x, -p). \tag{B.16}$$

To summarize, we have found, starting from basic physical considerations

$$\mathcal{P} : x_i \to -x_i \quad p_i \to -p_i \tag{B.17}$$

$$\mathcal{T} : x_i \to \quad x_i \quad p_i \to -p_i \quad \mathrm{i} \to -\mathrm{i}. \tag{B.18}$$

These were previously stated in the introduction.

Bibliography

[1] Bender, C.M., B.K Berntson, D. Parker, and E. Samuel. Observation of $\mathcal{PT}$ phase transition in a simple mechanical system. Am. J. Phys. (to appear). `arXiv:math-ph/1206.4972`.

[2] Bender, C.M., D.C. Brody, L.P Hughston, and B.K. Meister. Geometry of $\mathcal{PT}$-symmetric quantum mechanics.

[3] Bender, C.M., S. Boettcher, and P.N. Meisinger. $\mathcal{PT}$-symmetric quantum mechanics. J. Math. Phys. 40, 2201. 1999.

[4] Bender, C.M., D.C. Brody, and H.F. Jones. Complex Extension of Quantum Mechanics. Phys. Rev. Lett. 89, 270401. 2002.

[5] Bender, C.M. and S. Boettcher. Real Spectra in Non-Hermitian Hamiltonians Having $\mathcal{PT}$ Symmetry. Phys. Rev. Lett. 80, 5243. 1998.

[6] Schinder, J. et. al. Experimental Study of Active LRC Circuits with $\mathcal{PT}$-Symmetries. Phys. Rev. A 84, 040101. 2011.

[7] Berntson, B.K. Analysis of a Hydrogen Atom Analgoue in Non-Euclidean Space of Constant Curvature using Superingrability Methods. Proceedings of the National Conference On Undergraduate Research (NCUR). 2011.

[8] Berntson, B.K. Analysis of Kepler-Type Problems in Non-Euclidian Geometries of Constant Curvature using Superintegrability Methods. University of Minnesota Honors Thesis. 2011.

[9] Mostafazadeh, A. Real Description of Classical Hamiltonian Dynamics Generated by a Complex Potential. Phys. Lett. A357, 177. 2006.

[10] Nakahara, M. Geometry, Topology and Physics. Second edition. Taylor and Francis. 2003.

[11] Shankar, R. Principles of Quantum Mechanics. Springer. 1994.

[12] Dimock, J. Quantum Mechanics and Quantum Field Theory: A Mathematical Primer. Cambridge University Press. 2011.

[13] Bender, C.M. and S.A. Orszag. Advanced Mathematical Methods for Scientists and Engineers: Asymptotic Methods and Perturbation Theory. Springer. 1999.

[14] Rüter, C.E, K. Makris, R. El-Ganainy, D.N. Christodoulides, M. Segev, and D. Kip. Observation of parity-time symmetry in optics.

[15] Zhao, K.F., M. Schaden, and Z. Wu. Enhanced magnetic resonance of spin-polarized Rb atoms near surfaces of coated cells. Phys. Rev. A 81, 042903. 2010.

[16] Feng, L. et. al. Nonreciprocal Light Propagation in a Silicon Photonic Circuit. Science 333, 6043. 2011.

[17] Rubinstein, J., P. Sternberg, and Q. Ma. Bifurcation Diagram and Pattern Formation of Phase Slip Centers in Superconducting Wires Driven with Electric Currents. Phys. Rev. Lett. 99, 167003. 2007.

[18] Guo, A., G.J. Salamo, D. Duchesne, R. Morandotti, M. Volatier-Ravat, V. Aimez, G.A. Siviloglou, and D.N. Christodoulides. Observation of $\mathcal{PT}$-Symmetry Breaking in Complex Optical Potentials. Phys. Rev. Let.. 103, 093902. 2009.

[19] Bittner, S. et. al. PT symmetry and spontaneous symmetry breaking in a microwave billiard. Phys. Rev. Lett. 108, 024101. 2012.

[20] Dorey, P., C. Dunning, and R. Tateo. Spectral equivalences, Bethe Ansatz equations, and reality properties in $\mathcal{PT}$-symmetric quantum mechanics.

[21] Bender, C.M. and A. Turbiner. Analytic continuation of eigenvalue problems. Phys. Lett. A 173, 442. 1993.

[22] Pike, E.R. and S. Sarkar. The Quantum Theory of Radiation. Clarendon Press. 1995.

[23] Bender, C.M. and S. Kuzhel. Unbounded $\mathcal{C}$ symmetries and their nonuniqueness. arXiv:quant-ph/1207.1176

[24] Bender, C.M., P.N. Meisinger, and Q. Wang. Calculation of the Hidden Symmetry Operator in PT-Symmetric Quantum Mechanics. J. Phys. A: Math. Gen. 36, 1973. 2003.

[25] Wang, Q. Calculation of $\mathcal{C}$ Operator in $\mathcal{PT}$ -Symmetric Quantum Mechanics. Proceedings of Institute of Mathematics of NAS of Ukraine. 2003.

[26] Mostafazadeh, A. Pseudo-supersymmetric quantum mechanics and isospectral pseudo-Hermitian Hamiltonians. Nucl. Phys. B640, 419. 2002.

[27] Langer, H. and C. Tretter. A Kreĭn space approach to $\mathcal{PT}$-symmetry. Czech. J. Phys 54, 1113. 2004.

[28] Pontryagin, L.S. Hermitian operators in spaces with indefinite metrics. Bull. Acad. Sci. URSS. Ser. Math. 8, 243. 1944.

[29] Kreĭn, M.G. An intrroduction to the geometry of indefinite J-spaces and theory of operators in these spaces. Proc. Second Math. Summer School, Part I. 15. 1965.

[30] Bender, C.M. and D.W. Darg. Spontaneous Breaking of Classical $\mathcal{PT}$ Symmetry. J. Math. Phys. 48, 042703. 2007.

[31] Bender, C.M. and D. Hook. Quantum tunneling as a classical anomaly. J. Phys. A: Math. Theor. 44, 37. 2011.

[32] Arpornthip, T. and C.M. Bender. Conduction bands in classical periodic potentials. Pramana J. Phys. 73, 259. 2009.

[33] Bender, C.M., D.W. Hook, P.N. Meisinger, and Q. Wang. Complex Correpsondence Principle. Phys. Rev. Lett. 104, 061601. 2010

[34] Bender, C.M., M. Moshe, and S. Sarkar. Resolution of Inconsistency in the Double-Scaling Limit. arXiv:hep-th/1206.4943 . 2012.

[35] Moffat, J.W. Can Electroweak Theory Without a Higgs Particle be Renormalizable? arXiv:hep-ph/1109.5383. 2011.

[36] Mannheim, P.D. Astrophysical evidence for the non-Hermitian but PT-symmetric Hamiltonian of conformal gravity. Fortschr. Phys.. doi: 10.1002/prop.201200100. 2012.

[37] Gomez-Ullate, D., P. Santini, M. Sommacal, and F. Calogero. Understanding complex dynamics by means of an associated Riemann surface. `arXiv:nlin.CD:1104.2205`. 2011.

[38] Mostafazadeh, A. Pseudo-Hermitian Quantum Mechanics with Unbounded Metric Operators. Phil. Trans. R. Soc. A, (to appear). `arXiv:math-ph/1203.6241`

[39] Mostafazadeh, A. Pseudo-Hermiticity versus $\mathcal{PT}$-Symmetry: The necessary condition for the reality of the spectrum of a non-Hermitian Hamiltonian. J. Math. Phys. 43, 205. 2002.

[40] Mostafazadeh, A. Pseudo-Hermiticity versus $\mathcal{PT}$-Symmetry II: A complete characterization of non-Hermitian Hamiltonians with a real spectrum. J. Math. Phys. 43, 2814. 2002.

[41] Mostafazadeh, A. Pseudo-Hermiticity versus $\mathcal{PT}$-Symmetry III: Equivalence of pseudo-Hermiticity and the presence of antilinear symmetries. J. Math. Phys. 43, 3944. 2002.

[42] Mostafazadeh, A. Pseudo-Hermiticity and Generalized $\mathcal{PT}$- and $\mathcal{CPT}$-Symmetries. J. Math. Phys. 44, 974. 2003.

[43] Goldstein, H., C. Poole, and J. Safko. Classical Mechanics. Third edition. Addison Wesley. 2002.

[44] Huggett, S.A. and K.P. Tod. An Introduction to Twistor Theory. Cambridge University Press. 1994.

[45] Arnold, V.I. Mathematical Methods of Classical Mechanics. Second edition. Springer. 1989.

[46] Peskin, M.E. and D.V. Schroeder. An Introduction to Quantum Field Theory. Westview Press. 1995.

[47] Donaldson, S. Riemann Surfaces. Oxford University Press. 2011.

[48] Allen, L. and J. H. Eberly, Optical Resonance and Two-Level Atoms Dover. 1987.

[49] Bender, C.M., S. Boettcher, and V.M. Savage. Conjecture on the Interlacing of Zeros in Complex Sturm-Liouville Problems. J. Math. Phys. 41, 6381. 2000.

[50] Deatils of the cideo camera system: Single user VisiLog, full version with advanced USB video camera and gooseneck stand. Supplied by 2012 ScienceScope.